Resident Synovial Macrophages in Synovial Fluid: Implications for Immunoregulation in Infectious and Inflammatory Arthritis

Karen I. Cyndari, MD, PhD[1,2], Breanna M. Scorza, PhD[2,3], Zeb R. Zacharias, PhD[4,5], Leela Strand[6], Kurayi Mahachi, MPH, PhD[7], Juan Marcos Oviedo, PhD[8], Lisa Gibbs, BS[8], Danielle Pessoa-Pereira, PhD[2,3], Graham Ausdal, MPH[2,3], Dylan Hendricks, MS[2,3], Rika Yahashiri[9], Jacob M. Elkins, MD, PhD[10], Trevor Gulbrandsen, MD[10], Andrew R. Peterson, MSPH, MD[10], Michael C. Willey, MD[10], Keke C. Fairfax, PhD[8,] and Christine A. Petersen, DVM, PhD[2,3]

[1]Department of Emergency Medicine, University of Iowa, Iowa City, IA
[2]Center for Emerging Infectious Diseases
[3]Department of Epidemiology, University of Iowa, Iowa City, IA
[4]Human Immunology Core, University of Iowa, Iowa City, IA
[5]Holden Comprehensive Cancer Center, Iowa City, IA
[6]North Liberty High School, North Liberty, IA
[7]Research and Analytics, Enterprise Analytics, Sentara Health
[8]Department of Pathology, University of Utah, Salt Lake City, UT
[9]Williams College, Williamstown, MA
[10]Department of Orthopedics, University of Iowa, Iowa City, IA

Sources of funding:
Cyndari: This project was supported by funding from the Herbert N. Hultgren Award (Wilderness Medicine Society), the University of Iowa Physician-Scientist Training Program, and the University of Iowa Department of Emergency Medicine.

Corresponding Author:
Karen Cyndari, MD, PhD
Tel: 585-797-3464
karen-cyndari@uiowa.edu

University of Iowa Hospitals and Clinics
200 Hawkins Drive
1008 RCP
Iowa City, IA 52242

Keywords: resident synovial macrophage, Type A synoviocyte, joint space immunoregulation, septic arthritis, inflammatory arthritis

Abstract:

Objectives: Resident synovial macrophages (RSM) provide immune sequestration of the joint space and are likely involved in initiation and perpetuation of the joint-specific immune response. We sought to identify RSM in synovial fluid (SF) and demonstrate migratory ability, in additional to functional changes that may perpetuate a chronic inflammatory response within joint spaces.

Methods: We recruited human patients presenting with undifferentiated arthritis in multiple clinical settings. We used flow cytometry to identify mononuclear cells in peripheral blood and SF. We used a novel transwell migration assay with human *ex-vivo* synovium obtained intra-operatively to validate flow cytometry findings. We used single cell RNA-sequencing (scRNA-seq) to further identify macrophage/monocyte subsets. ELISA was used to evaluate the bone-resorption potential of SF.

Results: We were able to identify a rare population of $CD14^{dim}$, OPG^{+}, $ZO\text{-}1^{+}$ cells consistent with RSM in SF via flow cytometry. These cells were relatively enriched in the SF during infectious processes, but absolutely decreased compared to healthy controls. Similar putative RSM were identified using *ex vivo* migration assays when MCP-1 and LPS were used as migratory stimulus. scRNA-seq revealed a population consistent with RSM transcriptionally related to $CD56^{+}$ cytotoxic dendritic cells and IDO^{+} M2 macrophages.

Conclusion: We identified a rare cell population consistent with RSM, indicating these cells are likely migratory and able to initiate or coordinate both acute (septic) or chronic (autoimmune or inflammatory) arthritis. RSM analysis via scRNA-seq indicated these cells are M2 skewed, capable of antigen presentation, and have consistent functions in both septic and inflammatory arthritis.

Introduction: Damage to the articular surface of joints resulting in arthritis may be secondary to infection, inflammation, and chronic or acute trauma. Different etiologies of arthritis result in unique local immune environments within the joint space, but also systemically. While healthy synovium delineates an immune-privileged space to which few circulating cells gain entry (1), there are significant numbers of immune cells in the synovial fluid of pathologic joints (2; 3; 4). This indicates the localized synovial immune response is coordinated by the synovium itself, which can limit entry to the synovial fluid by actively sequestering or “cloaking” inflammatory damage (5) versus allowing circulating immune cells to enter synovial fluid.

The synovium is primarily composed of two types of cells: Fibroblast-like Synoviocytes (FLS) and Resident Synovial Macrophages (RSM), otherwise known as Type A cells or Tissue Resident Macrophages. FLS exist in the synovial intimal lining, express MHC Class II, and produce lubricating joint fluid, including hyaluronan (6). In pathologic settings, FLS are involved in joint inflammation and, ultimately, cartilage destruction (6). Conversely, RSM compose approximately 10% of the synovial lining, and to date have only been identified using direct tissue histology. Resident macrophages have previously been described *in situ* as constitutively anti-inflammatory (5), as opposed to circulating monocytes, which may either assist with sequestration of pathology or provide further momentum toward significant cellular collateral damage (5).

It was recently discovered that RSM are derived from embryonic precursor cells and perpetuate through self-proliferation within synovium (7). Certain cellular surface receptors, chemokines, or structural proteins such as CD68, osteoprotegerin (OPG/TNFRSF11B), CX3CR1, ZO-1/TJP1, F11R/JAM-A/JAM-1/CD321, and Triggering

Receptor Expressed on Myeloid cells 2 (TREM2) (8; 7) have all been proposed to identify these cells in differing circumstances, yet it remains difficult to differentiate RSM from macrophages and monocytes recruited from circulation. RSM have not been further evaluated in synovial fluid as it is unclear if they are able to migrate into the joint space to interact with, for example, T cells or Natural Killer (NK) cells, or if they remain synovial tissue resident cells only. As inflammation has been shown to immediately dysregulate tight junctions connecting these epithelial-like RSM (7), it is possible that these cells could leave the synovium and participate in joint space immune responses.

Here, we have identified RSM in synovial fluid from healthy, inflamed, and septic joints using flow cytometry and single cell RNA sequencing (scRNA-seq). We describe a subset of $CD14^{dim}$OPG+ZO-1+ M2 macrophages enriched in synovial fluid of pathologic joints consistent with previously published histological descriptions of RSM. *Ex vivo* migration experiments validated the migration of these cells from tissue. Single cell analysis reveals these putative RSM have dysregulated complement in settings of inflammatory arthritis, and a unique Reactome signature involving niacin and thiamine metabolism. This work is important in understanding how damage to the joint space is initiated and perpetuated both during infectious and inflammatory arthritis.

Materials and Methods:

Patient Recruitment: These studies were approved by the Institutional Review Board (IRB) at the University of Iowa Hospitals and Clinics. For synovial fluid studies, patients were recruited if they were being evaluated for septic arthritis. Exclusion criteria included recent significant trauma to the joint, immunomodulatory medications, or recent

joint replacement in the affected joint(s) (<1 year). All patients provided a blood sample. Not all patients required or had successful arthrocentesis. For those patients with synovial fluid sample, classification of Normal, Non-Inflammatory, Inflammatory, or Septic arthritis was based on established guidelines in orthopedics and rheumatology (9). For synovium procurement, 6 patients >18 years of age receiving a scheduled, non-emergent, total joint replacement or resection arthroplasty secondary to infection were recruited. Joint tissue consistent with synovium (knee) or pulvinar (hip) was sterilely obtained during normal operating protocol and did not alter the course of procedure.

PBMC and Synovial Fluid Cell Sample Preparation: Peripheral blood mononuclear cells (PBMCs) were isolated from whole blood over Ficoll-Paque PLUS (Cytiva, Fisherbrand). PBMCs were counted and cryopreserved in 90% FBS with 10% DMSO until analysis. For synovial fluid samples, a 200 µl aliquot was centrifuged at 1000 relative centrifugal force (RCF) for 10 minutes and stored at -80°C for ELISA. The remainder of the SF was treated with bovine testes hyaluronidase (Sigma-Adritch) according to manufacturer's synovial fluid clarification protocol. Synovial fluid was then filtered through a 70µm nylon mesh strainer (Fisher Scientific). SF was then diluted to 10 mL with PBS and centrifuged at 400 RCF for 10 minutes at room temperature. Supernatant was discarded. SF cells were counted and then cryopreserved in 90% FBS with 10% DMSO.

Transwell Migration Assay: Tissue acquired in the operating room was transferred to the laboratory in PBS on ice. Whole synovium was washed twice in PBS, then sterilely dissected into 4x4 mm segments, and washed again. Segments were placed into 24-well transwell inserts with 5 µm pores (Corning), a size that should allow monocyte and

macrophage migration, but prevent fibroblast migration (10). Bottom wells were treated with LPS (1, 10, or 100 µg/mL, Sigma-Aldrich) or MCP-1 (25 ng or 250 ng/mL, Fischer Scientific) in DMEM supplemented with 10% FBS and 1% penicillin/streptomycin. The inserts were then placed in the well, and enough media to cover the tissue was placed in the insert (approximately 200-400 µl). The transwell plates were incubated for 24 hours at 37°C and 5% CO_2. After incubation, the cells in the bottom well media were counted, and a crystal violet assay was performed on cells adhered to the bottom of the well and the underside of the transwell per standard protocol. Migratory cells in solution were analyzed using flow cytometry.

Flow Cytometry Analysis: For RSM analysis, samples of SF cells and PBMC were thawed in a water bath at 37°C, transferred into 10 mL of ice-cold PBS, pelleted at 400 RCF for 10 minutes at 4°C, and resuspended in ice-cold PBS. These samples were plated in a 96-well plate for single stain, Fluorescence Minus One (FMO), unstained, and patient test samples. Controls were plated at $2x10^5$ cells per well, and patient test samples at $1\text{-}2x10^6$ cells per well. Fluorochromes, targets, vendors, and lineage markers are listed in **Supplemental Table 1**. For intracellular staining (OPG, CD68, F11R/CD321, TREM2, ZO-1 and RANKL), cells were fixed and permeabilized with Fixation Buffer and Intracellular Staining Perm Wash Buffer (BioLegend) or Cytofix/Cytoperm Fixation/Permeabilization Solution Kit (BD Bioscences) according to manufacturer's protocol. Flow Cytometry gating strategy for patient SF and PBMC samples shown in **Supplemental Figure 1**. Gating strategy for transwell migration assay shown in **Supplemental Figure 2**. Flow cytometry was performed on a Cytek

Aurora cytometer (Bethesda, MD) located in the University of Iowa Flow Cytometry Core facility. Analysis was performed using FlowJo (Ashland, OR) software.

Enzyme-linked Immunosorbent Assays: Human TIMP-1 (RAB0466-1KT), TGF-BETA (RAB0460-1KT), TRACP (RAB1755-1KT), OPG/TNFRSF11B (RAB0484-1KT), IFN GAMMA (RAB0222-1KT), TNF-ALPHA (RAB0476-1KT), MMP-9 (RAB0372-1KT) and BMP2 (RAB0028-1KT) ELISA kits were obtained from Millipore Sigma, and sRANKL (MBS262624) kit from MyBioSource. For TIMP-1 and MMP-9, SF was diluted 1:500, for sRANKL dilution was 1:100, and all others were diluted 1:20. TGF-β1 was activated and then neutralized per manufacturer's protocol. Plates were read using a VERSAmax plate reader (Molecular Devices) and analyzed using MyAssays.com, Microsoft Excel, and GraphPad Prism 9.4.1.

Cell Sorting: To prepare the highest quality sample for single cell RNA sequencing (scRNA-seq), patients who had the highest percentage of viable, non-neutrophil cells in synovial fluid as seen by flow cytometry were selected, with 3 patients meeting criteria for septic arthritis, and 3 patients meeting criteria for inflammatory arthritis, regardless of crystal status. As SF in non-pathologic states lacks sufficient cellularity for scRNA-seq analysis, control patients were not included in analysis. Banked SF cell samples were thawed in a 37ºC water bath and immediately diluted in 4 mL Fluorescence Activated Cell Sorting (FACS) buffer and centrifuged at 4ºC at 1400 rpm. Supernatant was gently decanted, and cells resuspended in 50 µL of ice cold FACS buffer. Cells were then stained with 5 µl/reaction of CD244/APC (Clone C1.7), CD11b/BV695 (Clone ICRF44), CD66b/FITC (Clone G10F5) and CD56/PE (Clone 5.1H11), all from BioLegend. Cells were additionally stained with DAPI at 1:1000. Cells were incubated in the dark at 4ºC

for 30 minutes, washed once in ice cold FACS buffer, and resuspended in 50 µL of FACS buffer. Samples were then sorted on a Sony MA900 (San Jose, CA) with 100 µm sorting chip, sorting out $CD66b^+$ and DAPI positive cells, then sorting on $CD11b^+$, $CD56^+$, or $CD244^+$ positive cells into tubes containing cold PBS with 1% BSA. Cells were then counted for viability using trypan blue on a hemocytometer and concentrated according to 10X Chromium 3' kit guidelines.

Single Cell RNA sequencing: Cells were delivered to the Sequencing Core at the University of Utah, where RNA library generation was performed on a 10X Chromium Controller according to manufacturer's guidelines. RNA libraries were then sent to NovoGene (Sacramento, CA) for sequencing. Analysis was performed in RStudio with R v4.2.2 using Seurat (11; 12; 13; 14), ReactomeGSA (15) and EnhancedVolcano (16). MT-DNA percentage was limited to 15% during quality control analysis (17). The number of unique genes was set as 200 to 5000. A minimum of 3 cells were required to express each gene. Data was normalized using a global-scaling normalization method per Seurat with a scale factor of 10,000 with log transformation, then the data was integrated into a single database. A resolution of 0.4 was used to define clusters with dimensions set 1:30. Clusters were annotated by identifying top 10 gene expression in addition to expression of markers such as CD56, MRC1/CD206, F11R, and CD68. Log2FC threshold was set to 0.5 for gene expression. Analysis was performed comparing septic arthritis (n=3 patients) to inflammatory arthritis (n=3 patients). Adjusted p-values were used to determine significance of Differentially Expressed Genes (DEGs), with Log2FC threshold was 1.5 given the homogenous sample. For Conserved Markers, included genes had min.diff.pct set to 0.7, and min.pct to 0.25.

Statistics: Descriptive statistics were used to compare patient demographics and underlying diagnoses. Statistical analysis was performed using GraphPad Prism v9.4.1. Flow Cytometry data was tabulated in FlowJo, and 2-way ANOVA with Tukey's *post-hoc* correction was used to compare %parent or %total cells of control, inflammatory, and septic arthritis populations. Mann-Whitney U-tests were used to compare ELISA results between the 3 arthritis groups (control, inflammatory, and septic). DEG and Conserved gene analysis was performed in Seurat per individual cell cluster using adjusted p-values.

Results:

Patient Demographics: To identify Resident Synovial Macrophages (RSM) in synovial fluid (SF), 52 patients were recruited into the initial study. Of these, 32% of patients were female and 87% were Caucasian (**Table 1**). SF was obtained from 36 of 52 patients. Eighteen patients were found to have septic arthritis based on SF analysis and final culture results, and 8 had inflammatory arthritis. Of the remainder, 10 were designated non-inflammatory (<2000 WBCs) or normal (<200 WBCs) (**Supplementary Table 2**). All 52 patients provided peripheral blood samples for comparison to SF response.

Identification of Synovial Fluid Macrophages Consistent with Resident Synovial Macrophages: We identified a cell subset expressing myeloid marker CD11b, pan-macrophage marker CD68, anti-inflammatory macrophage marker TREM2 (18), Major Histocompatibility Complex marker Class II HLA-DR (19), CX3CR1 (7), OPG (19), and

hematopoietic/macrophage adhesion marker CD45 (20). These cells were also negative for Receptor Activator of NF-kB Ligand/RANKL (19) and for the dendritic cell marker CD11c. These cells formed two distinct subpopulations: a $CD14^{hi}$ and a $CD14^{dim}$ population (**Figure 1A**). The $CD45^{+}CD14^{dim}$ RSM-like population was evaluated in inflammatory and septic arthritis patients and found to have an absolute decrease in frequency compared to control SF cells (**Figure 1B**). However, these cells were relatively enriched in SF compared to the PBMC fraction (**Figure 1C**). The Alive/ $CD45^{+}CD14^{dim}$ was then back-gated to better describe this population, first to evaluate how many of these cells were macrophages by CD68 and TREM2, then if these macrophages also co-expressed RSM markers OPG and ZO-1 (**Figure 1D**). For patients with inflammatory arthritis, 1.96% of the $CD14^{dim}$ cells were macrophages, and of those macrophages, 34.35% were RSM-like by OPG and ZO-1 expression. For patients with septic arthritis, 0.92% of $CD14^{dim}$ cells were macrophages, and of those 9.97% were RSM-like.

Identification of RSM-like Cells Migrating from Intact Synovium: We obtained synovium from patients undergoing total joint replacement or resection arthroplasty. The inner membrane of the joint space was carefully dissected and placed as intact explants into transwells (**Figure 2A**). The migratory synovial myeloid population (Live/$CD56^{-}$/$CD3^{-}$/$CD11c^{-}$/$CD20^{-}$/$CD14^{+}$/$CD11b^{+}$) in a representative patient sample contained OPG+, TREM-2+, ZO-1+, CX3CR1+, and F11R+ populations in the lower transwell media (**Figure 2B**). Sixty-five percent of CD11b+$CD14^{dim}$ cells migrating out of the synovium tissue were double positive for OPG and CX3CR1, and of those cells, 93.8% were double positive for tight junction markers F11R and ZO-1. However, we noted the

CD14^{hi} macrophages displayed the greatest increase in the proposed RSM markers (**Figure 2B**), and the relevance of CD14dim versus high in the acute *ex vivo* setting requires further clarification. To evaluate co-expression of these RSM-specific markers, t-distributed Stochastic Neighbor Embedding (tSNE) plots were created. Of the synovial myeloid population described above, there was weak or low expression of all RSM-specific markers, but ZO-1 may be most specific to identifying migratory RSM in SF (**Figure 2C, top right**). Cells with markers of circulating immune subsets, including neutrophils (CD66b), NK cells (CD56), and T cells (CD3) were also present in the lower transwell chambers (**Supplemental Figure 3)**. Though there were no significant differences found between treatments in this experiment, in all cases the stimuli resulted in decreased levels of putative RSM migration compared to control, indicating these RSM may remain active in the tissue, and migratory cells present in the control may be in response to tissue trauma, an effect that is countered by the stimuli. Cells found adhered to the underside of the transwell or in the bottom of the lower well were below the limit of detection by Crystal Violet assay (data not shown). Therefore, we conclude that RSMs can migrate out of the synovium, and ZO-1 is likely the most specific RSM marker expressed by myeloid cells, but tight junction markers in conjunction with M2 markers and OPG are necessary for identification.

Evaluation of Pro and Anti-Resorptive Potential of Synovial Fluid: SF supernatant was analyzed for cytokines that are implicated in bone and/or cartilage destruction. OPG is the decoy receptor for RANKL, which in turn is required for the formation of osteoclasts; the ratio between these two cytokines is an important method to evaluate

bone maintenance versus destruction (**Figure 3A**) (21). **Figure 3B** evaluates the role of other osteo-relevant and immunomodulatory cytokines. The collagenase Tartrate Resistant Acid Phosphatase (TRAP), which is secreted by osteoclasts, had no observed change. Transforming Growth Factor Beta (TGF-β) not only inhibits osteoclastogenesis (22), but also stimulates osteoblasts (23) and further, it is stored in the latent phase within the extracellular matrix to be released during bone turnover (24; 25). Likewise, there was no significant difference between pathologic SF and control TGF-β levels. We also tested Bone Morphogenic Protein 2 (BMP2), TNF-α and IFN-γ. BMP2 induces osteoblast differentiation and TNF-α and IFN-γ are well established pro-inflammatory cytokines that result in osteoclast activation and inhibition, respectively (26; 22). All were below the limit of detection (data not shown) in all patient groups. Finally, Tissue Inhibitor of Matrix Metalloproteinases 1 (TIMP1) and Matrix Metallopeptidase 9 (MMP9) were evaluated (**Figure 3C**). TIMP1 is an inhibitor of MMPs. MMP9 is expressed by osteoclasts and is an important enzyme for bone remodeling (27). There was an increase in MMP9 in patients with inflammatory and septic arthritis, and a significantly decreased ratio of TIMP1: MMP9 in these patients as well (**Figure 3C, right**). Therefore, there is increased potential for bone and cartilage damage in patients with inflammatory and septic arthritis due mainly to increased MMP9, which is possibly due to increased osteoclastogenesis secondary to increased RANKL, or increased synovial fibroblast production. As RSM-like cells were decreased in SF of septic arthritis patients that also had highest RANKL and MMP9, it is possible RSM provide a protective mechanism against bone and joint destruction. The specific cytokine production profile of RSM specifically will require further evaluation.

Identification of Rare Cell Subsets Using Single Cell RNA-Sequencing: The results of SF RSM flow cytometry and the potential for bone damage implicated by SF ELISA results led us to evaluate the functional transcriptome profile of rare cell populations using scRNA-seq. First, we analyzed for highly variable features, demonstrating a relevant focus of M1 and M2 functions (**Supplemental Figure 4A**). Putative monocyte/macrophage and NK/NKT cell subpopulations were clustered into 11 groups (**Figure 4A**) with manual annotation of the clusters based on top ten gene expression (**Figure 4B**). There were not enough cell events to separately cluster NK and NKT cells, therefore they are represented in a single, though spatially separate, cluster.

After assigning known and widely accepted monocyte/macrophage designations based on gene profiles, clusters 9 and 10 were not able to be assigned a known designation. Cluster 10 expressed NK-marker *CD56* (Log2FC 0.64) and low *CD68* (Log2FC -2.07) (**Supplementary Figure 4B**), while also having high *HLA* expression (**Figure 4B**). Therefore, we putatively classified this cluster as a cytotoxic or “killer” dendritic cell population (28). Cluster 9 expressed tight junction protein *F11R/JAM1* (7), macrophage marker *CD68,* and M2-marker *IDO1* (29) (**Figure 4B, Supplementary Figure 4B**). This is consistent with the RSM phenotype. As expected, the proposed RSM population was rare in comparison to well-studied subpopulations designated by clusters 0-7. *ZO-1/TJP1* (7) was not represented in any cluster, and *OPG/TNFRSF11B* was minimally expressed, but only in Cluster 9. This is contrary to flow cytometry findings and may represent decreased mRNA expression regardless of current protein expression. We also evaluated expression of resident macrophage transcription factor

GATA6 (30), which was minimally expressed, but only in Cluster 3. This may indicate that RSMs are split between multiple clusters, as Cluster 3 was designated as Dendritic Cells based on high expression of HLA—which is also consistent with sub-intimal RSM, but not intimal RSM (8). Based on PCA analysis (**Supplemental Figure 4C**), putative cytotoxic DCs were more closely related to NK/NKT cells than to RSM, and the cytotoxic DC and RSM populations may represent phases of differentiation of the same cell of origin, as both were distinct from the circulating monocyte/macrophage population. The plasticity of tissue macrophages, and ability to survive in new compartments has been both advocated and challenged (31), and the exact lineage remains unknown.

Differentially Expressed Genes (DEGs) were explored using a volcano plot (**Supplemental Figure 4D**) and a Log2FC threshold of 1.5 due to the homogeneous cell populations (e.g., nearly all myeloid) being compared. Using this criterion, DEGs were found to be statistically significant in Clusters 0-8 (**Figure 5**). Transcripts highly upregulated in septic arthritis (and therefore down-regulated in inflammatory arthritis) among multiple clusters included *HLA-DRB5, C15orf48, IL1B, AC025580.2*, and *SOD2*. In inflammatory arthritis, common gene upregulation included *PPARG, FABP5, CD36*, *NLRP3, SPP1, and MITF*. M1 macrophages from the two different arthritis etiologies showed a distinctly different gene expression patterns with an upregulation of *GBP1, GBP5*, and *TIMP1.*

Conserved genes that remained highly expressed in both inflammatory and infectious arthritis were also examined, as these could represent novel targets in the treatment, or prevent the conversion of infectious to inflammatory arthritis. Conserved

genes were only significant in DC, NK/NKT, RSM, and Cytotoxic DC clusters (**Figure 6, Supplementary Table 4**). Nearly all genes were associated with cytolytic function, antigen presentation, M1/M2 polarity, or lysosomes.

Gene Set Analysis (GSA) was then assessed to determine the overall, broad picture, of cell function and metabolism (**Figure 7**) with the 15 most upregulated or downregulated pathways comparing septic arthritis to inflammatory arthritis, which identified complement (lectin pathway in septic arthritis, and classical pathway in inflammatory arthritis), bone-derived FGF23 signaling (FCFR1c and klotho ligand binding (32), and COX signaling. Pathways related specifically to immune function were further evaluated immune-relevant (**Figure 8A**), related to phagocytic potential (**Figure 8B**), complement (**Figure 8C**) and adhesion (**Figure 8D**). In phagocytic and complement context, Cytotoxic DC, NK/NKT, and RSMs populations shared a similar pattern compared to all other clusters, indicating functional overlap between these subpopulations. This pattern was only disrupted when evaluating for cell adhesion/polarity, where phylogeny indicates RSMs and M2 monocytes are most similar in function. GSA was further performed specifically on the RSM cluster to identify the maximum changes in septic and inflammatory arthritis (**Supplementary Figure 5**), which identified threonine, pyridoxine, and thiamine metabolism.

Discussion:

Resident Synovial Macrophages are regulatory immune cells of the joint space that have traditionally been identified only in tissue using histology. In this manuscript, we reveal a rare subset of macrophages identified by flow cytometry in SF consistent

with previously described RSM, with a phenotype indicating migratory capacity, especially during pathologies that dysregulate tight junctions. The role of these cells in SF has yet to be established.

Though CX3CR1 was found to be specific for RSM within murine synovial tissue previously (1), we were not able to use this chemokine receptor to distinguish SF cells from peripheral monocytes (33). Likewise, HLA-DR expression has been shown to be downregulated in the intimal-lining RSMs, but upregulated in sub-intimal RSMs (8), and it is unclear if HLA-DR expression would assist in identification of RSM-like cells in the SF. Further, we first identified putative RSM as $CD14^{dim}$, M2 macrophages expressing OPG. $CD14^{dim}$ monocytes have been well described previously as non-classical and poorly phagocytic (34; 35), however data is limited on $CD14^{dim}$ macrophages. $CD14^{dim}$ gingival macrophages were found to be M2/anti-inflammatory and likely osteo-protective by high expression of IL-10 and TGF-β in the setting of gingivitis (36). To fully elucidate the utility of CX3CR1, HLA-DR, and CD14 in human SF macrophage subsets requires further work.

To determine whether our identified cells came from synovium or from circulation, we piloted a novel transwell migration assay with human *ex vivo* synovium that validated our flow cytometry findings. Therefore, we believe the CD68/TREM2/OPG/ZO-1/F11R cell fraction is the most representative of putative RSMs. This explant model could be used widely to study other synovial pathology.

We then utilized scRNA-seq to identify a rare macrophage subpopulation consistent with transcriptional reports of RSMs, though markers identified using flow cytometry were not always identified in gene transcripts, including *ZO-1.* Rather, other

transcripts were identified, including M2/Tumor Associated Macrophage markers such as *IRF4* (37)*, IDO1* (38)*, TGFB1* and *IL10RB* (39) (**Supplemental Figure 4B**). While the presumed RSM cluster had characteristics of M2 macrophages, these cells also had a similar transcriptional signature to inflammatory NK/NKT and Cytotoxic DCs, indicating that RSMs may be capable of taking on an inflammatory and/or joint destructive phenotype in settings of chronic inflammation. This was demonstrated by the increase in M1 transcripts for *CCR7* (Log2FC 2.25) and co-stimulatory molecule *CD86* (Log2FC 0.92) in infectious settings (40).

To provide context to our findings, we compared our SF cell scRNA-seq to scRNA-seq performed on synovium. Human MERTK^{+}CD206^{+} RSM were found to be anti-inflammatory in patients in remission from rheumatoid arthritis (41). We found *MERTK* expressed highest in Cluster 5/M2 Monocytes (Log2FC 0.94), but it was not expressed in 9/RSM. Interestingly, MERTK^{-}CD206^{-} RSM indicated active rheumatoid arthritis disease (41). It is possible that given all patients who received arthrocentesis and participated in the scRNA-seq were acutely symptomatic that a MERTK^{+}CD206^{+} RSM profile was physiologically improbable. For *CD206/MRC1,* this was expressed highest in Cluster 4/M2 Macrophages, which additionally expressed *TREM2, FOLR2*, and *LYVE1* (41), though only *TREM2* had Log2FC >0.5. Once RSM leave the synovial tissue to enter the SF, previously established profiles may no longer applicable, and it is very possible that RSM may be distributed amongst clusters rather than a discrete cluster of their own. There is also significant plasticity in macrophages/monocytes, and monocyte precursors that migrate to the joint space may experience significant niche-specific differentiation.

Others found that RSM arose from CSF1R+ interstitial macrophages (7). We found *CSF1R* expressed in multiple other clusters, including 3-6, and 8-10. It was also found that interstitial RSM expressed *RETNLA, STMN1*, and *AQP1* (7). *RETNLA* and *AQP1* transcripts were not identified in this study, while STMN1 was only expressed by Cluster 3/DCs, but this was not significant. Likewise, markers of tight junctions and cell polarity previously found included *F11R, CLDN5, FAT4*, and *VANGL2*. Of these, only F11R was identified, and expressed mainly in RSM and Cytotoxic DC clusters (**Supplemental Figure 4B**).

We identified *LAMP3/CD208/DC-LAMP* as the top gene expressed by Cluster 9/RSM, and while the exact function of LAMP3 has yet to be elucidated, it is likely to be involved with MHC Class II peptide presentation (42). *LAMP3* is traditionally considered a marker of mature dendritic cells. Others have shown that DCs expressing LAMP3 are regulatory in nature and more enriched in draining lymph nodes rather than tumors (43). However, *LAMP3* is upregulated by THP-1 macrophages with *in vitro* LPS stimulation (44), and is constitutively expressed in primary macrophages in fish, chickens, and humans (45). *LAMP3* may have been induced in patients with septic arthritis like the aforementioned THP-1 cells with LPS stimulus. While the UMAP (**Figure 4**) shows Cluster 9/RSM and Cluster 3/DCs spatially close, the PCA analysis demonstrates larger differences (**Supplementary Figure 4C**). As SF cells were not examined under a microscope to determine the visual characteristics of DC versus macrophage, we conclude it is not possible to detangle the spectrum that is myeloid cell differentiation based only on gene expression.

Continuing analysis of Cluster 9/RSM gene expression, *ENOX1* was highly expressed (**Figure 4**) and is important for reduction of oxygen to superoxide, an essential macrophage function (46) (47). *CERS6* has been shown to contribute to mitochondrial dysfunction by promoting reactive oxygen species production in hepatocytes (48). *IDO1* expression in macrophages has been associated with increased immune cell infiltration and in squamous cell cancer (49) and colorectal cancer-associated macrophages (50). IDO1 specifically is involved with tryptophan metabolism, the metabolites of which inhibit oxidative cell death (51). Together this indicates that these cells are likely to have potent generation of superoxide, which may indicate that in infectious or inflammatory settings, RSM may perpetuate chronic inflammation. Until these RSM can be compared to similar cells from healthy SF, the baseline role and function are unclear.

Given we believe these cells are capable of migratory function, markers of migration and extravasation were also examined. CADM1 was highly and conservatively expressed by Cluster 9/RSM, and is strongly associated with TREM2+ tumor associated macrophages . *ALCAM* (Log2FC 0.73) is expressed by endothelial cells of the blood-brain barrier and monocytes that cross into this immune-privileged space (52), which may be consistent with the relative immune privilege of the joint space. In rheumatoid arthritis, ALCAM was also found expressed on granulocytes and monocytes within the SF (53). As ALCAM stabilizes tight junctions (54), this integrin may be important in the homeostasis of the joint space as maintained by RSM. *PECAM1* (Log2FC -1.03) assists with leukocyte migration through tight junctions (55). However, it remains unclear if the ALCAM and PECAM on endothelial cells, leukocytes,

or both, is essential for the presumed functions, as in knock out models, decreased function was not lineage specific. Our data seems to suggest a differential regulation of tight junctions by macrophages depending on pathology.

When we evaluated for DEGs between septic and inflammatory arthritis, RSM, Cytotoxic DC, and NK/NKT cells had none. This could be because these clusters have a more conserved function regardless of pathologic state, or because the number of cells analyzed was too low for significance given the rarity of these cells in SF—a rarity which was validated in direct tissue migration experiments. Regardless, the low percentage of this cell population and the difficulty acquiring SF samples is a limitation of this work. As there were no DEGs identified in Cluster 9/RSM, GSA was performed to identify unique pathways and discovered threonine, pyridoxine, and thiamine metabolism. The role of threonine catabolism is unclear in macrophages, but is critically necessary for murine stem cells viability (56), which may be similar function to locally renewing macrophage populations. Pyridoxine suppresses IL-1β release through NLRP3 inhibition (57), while thiamine precursors have been found to both increase cellular glutathione stores and inhibit NF-kB translocation to the nucleus in microglial cells (58), the resident macrophages of the brain. RSMs are upregulating anti-inflammatory pathways, but the question remains if the concurrent upregulation of complement genes may supersede the protective mechanisms in place through B vitamins, COX, and hydroxycarboxylic acid receptors.

We also evaluated the protein levels of multiple bone-relevant cytokines and related this to cell populations in the joint space. The DEG *TIMP1* was identified in Cluster 7/M1 Macrophage as highly upregulated in septic arthritis, with concurrent

downregulation in inflammatory arthritis. As a 1:1 inhibitor of MMP9 (59), TIMP1 is likely protective in the setting of joint inflammation by preserving the extracellular matrix of cartilage and bone from enzymatic degradation. We observed a decrease in the stoichiometric ratio of TIMP1:MMP9 protein concentration in both infectious and inflammatory arthritis SF, which is concerning for MMP9 as a major cause of bone destruction in these pathologic states, and a potential therapeutic target. *MMP9* was not differentially expressed, and MMP9 found by ELISA is likely from other cells, specifically fibroblast like synoviocytes and/or neutrophils (60), but possibly also osteoclasts (27). *TIMP1* was expressed in Cluster 9/RSM (Log2FC -2.67) indicating RSM would not be the primary source of this in SF.

In conclusion, the profile of a subset of M2, likely osteoprotective macrophages in SF that can be stimulated to migrate out of synovial tissue *ex vivo* suggests these are equivalent to tissue resident macrophages. However, these putative RSM expressed transcripts heavily involved with antigen presentation (LAMP3), oxidative stress (*ENOX1, CERS6, IDO1*), and cell migration (*ALCAM, PECAM*). This suggests that in settings of infectious or inflammatory arthritis, these cells may perpetuate rather than attenuate inflammation, and could be involved in the transition to chronic symptomology once out of the normal synovial tissue niche. Further work will focus on the cytokine expression of these putative migratory RSM, and the interactions of RSM with other cells in the joint space, including T cells, B cells, and NK or NKT cells.

Acknowledgements:

The authors would like to thank Catherine Fairfield BSN, EM Research Coordinator, and Alex Peebles, Cameron Williams, Shannon Landers, Klaudia Golebiewski, Allison Herr, Noble Briggs, Vanko Bicar, Malea Pinckney, Heath Gibbs, Nicole Grossmann, Scott Tibbetts, Ike Appleton, Jay Miller, and Jacob Hampton with the Emergency Department Research Enroller Program (ED-REP) for their essential role in enrolling patients and collecting data for this project.

The authors would also like to thank Dr. Daniel Livorsi and the Division of Infectious Diseases for assistance with patient recruitment.

The data presented herein were obtained at the Flow Cytometry Facility, which is a Carver College of Medicine / Holden Comprehensive Cancer Center core research facility at the University of Iowa. The facility is funded through user fees and the generous financial support of the Carver College of Medicine, Holden Comprehensive Cancer Center, and Iowa City Veteran's Administration Medical Center. Research reported in this publication was supported by: the National Center for Research Resources of the National Institutes of Health under Award Number 1 S10 OD034193-01; and the National Cancer Institute of the National Institutes of Health under Award Number P30CA086862

References

1. *Origin and function of synovial macrophage subsets during inflammatory joint disease.* **Culemann S, Grüneboom A, Krönke G.** 2019, Adv Immunol, Vol. 143, pp. 75-98.

2. *Immune cell profiles in synovial fluid after anterior cruciate ligament and meniscus injuries.* **Kim-Wang, S.Y., Holt, A.G., McGowan, A.M. et al.** 280, 2021, Arthritis Res Ther, Vol. 23.

3. *Synovial fluid monocyte/macrophage subsets and their correlation to patient-reported outcomes in osteoarthritic patients: a cohort study.* **Gómez-Aristizábal, A., Gandhi, R., Mahomed, N.N. et al.** 26, 2019, Arthritis Res Ther, Vol. 21.

4. *High percentages and activity of synovial fluid NK cells present in patients with advanced stage active Rheumatoid Arthritis.* **Yamin R, Berhani O, Peleg H, Aamar S, Stein N, Gamliel M, Hindi I, Scheiman-Elazary A, Gur C.** 1, 2019, Sci Rep, Vol. 9, p. 1351.

5. *Resident Macrophages Cloak Tissue Microlesions to Prevent Neutrophil-Driven Inflammatory Damage.* **Stefan Uderhardt, Andrew J. Martins, John S. Tsang, Tim Lämmermann, Ronald N. Germain,.** 3, 2019, Cell, Vol. 177, pp. 541-55.

6. *Fibroblast-like synoviocytes: key effector cells in rheumatoid arthritis.* **Bartok B, Firestein GS.** 1, 2010, Immunol Rev, Vol. 233, pp. 233-55.

7. *Locally renewing resident synovial macrophages provide a protective barrier for the joint.* **S, Culemann, et al.** 7771, 2019, Nature, Vol. 572, pp. 670-675.

8. *Critical Role of Synovial Tissue-Resident Macrophage and Fibroblast Subsets in the Persistence of Joint Inflammation.* **Kemble S, Croft AP.** 2021, Front Immunol.

9. *Synovial Fluid Tests: What Should Be Ordered?* **Shmerling RH, Delbanco TL, Tosteson ANA, Trentham DE.** 8, 1990, JAMA, Vol. 264, pp. 1009-1014.

10. **Corning Incorporated.** Transwell Permeable Supports Selection and Use Guide. 2013.

11. *Integrated analysis of multimodal single-cell data.* **Hao Y, Hao S, Andersen-Nissen E, III WMM, Zheng S, Butler A, Lee MJ, Wilk AJ, Darby C, Zagar M, Hoffman P, Stoeckius M, Papalexi E, Mimitou EP, Jain J, Srivastava A, Stuart T, Fleming LB, Yeung B, Rogers AJ, McElrath JM, Blish CA, Gottardo R, et al.** 2021, Cell.

12. *Comprehensive Integration of Single-Cell Data.* **Stuart T, Butler A, Hoffman P, Hafemeister C, Papalexi E, III WMM, Hao Y, Stoeckius M, Smibert P, Satija R.** 2019, Cell, Vol. 177, pp. 1888-1902.

13. *Integrating single-cell transcriptomic data across different conditions, technologies, and species.* **Butler A, Hoffman P, Smibert P, Papalexi E, Satija R.** 2018, Nature Biotechnology, Vol. 36, pp. 411-420.

14. *Spatial reconstruction of single-cell gene expression data.* **Satija R, Farrell JA, Gennert D, Schier AF, Regev A.** 2015, Nature Biotechnology, Vol. 33, pp. 495-502.

15. *ReactomeGSA - Efficient Multi-Omics Comparative Pathway Analysis.* **Griss J, Viteri G, Sidiropoulos K, Nguyen V, Fabregat A, Hermjakob H.** 2020, bioRxiv.

16. **Blighe K, Rana S, Lewis M.** EnhancedVolcano: Publication-ready volcano plots with enhanced colouring and labeling. [Online] https://github.com/kevinblighe/EnhancedVolcano.

17. *Systematic determination of the mitochondrial proportion in human and mice tissues for single-cell RNA-sequencing data quality control.* **Osorio D, Cai JJ.** 7, 2021, Bioinformatics, Vol. 37, pp. 963-967.

18. *Trem-2 Promotes Emergence of Restorative Macrophages and Endothelial Cells During Recovery From Hepatic Tissue Damage.* **Coelho Inês, Duarte Nádia, Barros André, Macedo Maria Paula, Penha-Gonçalves Carlos.** 2021, Frontiers in Immunology , Vol. 11.

19. *Synovial tissue macrophages: friend or foe?* **Kurowska-Stolarska M, Alivernini S.** 2017, RMD Open, Vol. 3, p. e000527.

20. *CD45 regulates Src family member kinase activity associated with macrophage integrin-mediated adhesion.* **Tamara Roach, Suzanne Salter, Michael Koval et al.** 6, 1997, Current Biology, Vol. 7, pp. 408-17.

21. *Biology of RANK, RANKL, and osteoprotegerin.* **Boyce BF, Xing L.** Suppl 1, 2007, Arthritis Res Ther, Vol. 9.

22. *Interferon-Gamma-Mediated Osteoimmunology.* **Tang M, Tian L, Luo G, Yu X.** 9, 2018, Front Immunol, Vol. 29, p. 1508.

23. *Role of transforming growth factor-beta in bone remodeling.* **Bonewald LF, Mundy GR.** 250, 1990, Clin Orthop Relat Res, pp. 261-76.

24. *The extracellular matrix and transforming growth factor-β1: Tale of a strained relationship.* **Hinz, Boris.** 2015, Matrix Biology, Vol. 47, pp. 54-65.

25. *TGF-β and BMP signaling in osteoblast, skeletal development, and bone formation, homeostasis and disease.* **Wu M, Chen G, Li YP.** 4, 2016, Bone Res, Vol. 26, p. 16009.

26. *Classical and Paradoxical Effects of TNF-α on Bone Homeostasis.* **Osta B, Benedetti G, Miossec P.** 5, 2014, Front Immunol, Vol. 13, p. 48.

27. *Matrix metalloproteinases in bone development and pathology: current knowledge and potential clinical utility.* **Liang HPH, Xu J, Xue M, Jackson CJ.** 2016, Metalloproteinases In Medicine, Vol. 3, pp. 93-102.

28. *CD56 marks human dendritic cell subsets with cytotoxic potential.* **Roothans D, Smits E, Lion E, Tel J, Anguille S.** 2, 2013, Oncoimmunology, Vol. 2, p. e23037.

29. *Critical role of synovial tissue-resident macrophage niche in joint homeostasis and suppression of chronic inflammation.* **Huang QQ, Doyle R, Chen SY, Sheng Q, Misharin AV, Mao Q, Winter DR, Pope RM.** 2, 2021, Sci Adv, Vol. 7, p. eabd0515.

30. *GATA6+ Peritoneal Resident Macrophage: The Immune Custodian in the Peritoneal Cavity.* **Jayakumar P, Laganson A, Deng M.** 866993, 2022, Front Pharmacol, Vol. 13.

31. *The expanding world of tissue-resident macrophages.* **Jenkins, S.J., and Judith E Allen.** 8, 2021, European Journal of Immunology, Vol. 51, pp. 1882-1896.

616 32. *Fibroblast growth factor 23 and bone mineralisation.* **Guo YC, Yuan Q.** 1, 2015, Int J Oral Sci, Vol. 7,
617 pp. 8-13.

618 33. *CX3CR1 is required for monocyte homeostasis and atherogenesis by promoting cell survival.* **Limor**
619 **Landsman, Liat Bar-On, Alma Zernecke, et al.** 4, 2009, Blood, Vol. 113, pp. 963-972.

620 34. *Human Monocyte Subsets and Phenotypes in Major Chronic Inflammatory Diseases.* **Kapellos**
621 **Theodore S., Bonaguro Lorenzo, Gemünd Ioanna, Reusch Nico, Saglam Adem, Hinkley Emily R.,**
622 **Schultze Joachim L.** 2019, Frontiers in Immunology , Vol. 10.

623 35. *Human CD14dim monocytes patrol and sense nucleic acids and viruses via TLR7 and TLR8 receptors.*
624 **Cros J, Cagnard N, Woollard K, Patey N, Zhang SY, Senechal B, Puel A, Biswas SK, Moshous D, Picard C,**
625 **Jais JP, D'Cruz D, Casanova JL, Trouillet C, Geissmann F.** 3, 2010, Immunity, Vol. 33, pp. 375-86.

626 36. *Macrophage subset sensitivity to endotoxin tolerisation by Porphyromonas gingivalis.* **Foey AD,**
627 **Crean S.** 7, 2013, PLoS One, Vol. 8, p. e67955.

628 37. *Interferon-regulatory factors determine macrophage phenotype polarization.* **Günthner R, Anders**
629 **HJ.** 2013, Mediators Inflamm, p. 731023.

630 38. *The role of indoleamine 2,3-dioxygenase (IDO) in immune tolerance: focus on macrophage*
631 *polarization of THP-1 cells.* **Wang XF, Wang HS, Wang H, Zhang F, Wang KF, Guo Q, Zhang G, Cai SH, Du**
632 **J.** 1-2, 2014, Cell Immunol, Vol. 289, pp. 42-8.

633 39. *TGF-β induces M2-like macrophage polarization via SNAIL-mediated suppression of a pro-*
634 *inflammatory phenotype.* **Zhang F, Wang H, Wang X, Jiang G, Liu H, Zhang G, Wang H, Fang R, Bu X, Cai**
635 **S, Du J.** 32, 2016, Oncotarget, Vol. 7, pp. 52294-52306.

636 40. *CD163 and CCR7 as markers for macrophage polarization in lung cancer microenvironment.* **Kwiecień**
637 **I, Polubiec-Kownacka M, Dziedzic D, Wołosz D, Rzepecki P, Domagała-Kulawik J.** 4, 2019, Cent Eur J
638 Immunol, Vol. 44, pp. 395-402.

639 41. *Distinct synovial tissue macrophage subsets regulate inflammation and remission in rheumatoid*
640 *arthritis. .* **Alivernini, S., MacDonald, L., Elmesmari, A. et al.** 2020, Nat Med, Vol. 26, pp. 1295-1306.

641 42. *Vitamin D3 regulates LAMP3 expression in monocyte derived dendritic cells.* **L. Malaguarnera, A.**
642 **Marsullo, K. Zorena, G. Musumeci, M. Di Rosa.** 2017, Cellular Immunology, Vol. 311, pp. 13-21.

643 43. *Mature dendritic cells enriched in immunoregulatory molecules (mregDCs): A novel population in the*
644 *tumour microenvironment and immunotherapy target.* **Li J, Zhou J, Huang H, Jiang J, Zhang T, Ni C.** 2,
645 2023, Clin Transl Med, Vol. 13, p. e1199.

646 44. *LAMP-3 (Lysosome-Associated Membrane Protein 3) Promotes the Intracellular Proliferation of*
647 *Salmonella typhimurium.* **Lee EJ, Park KS, Jeon IS, Choi JW, Lee SJ, Choy HE, Song KD, Lee HK, Choi JK.** 7,
648 2016, Mol Cells, Vol. 39, pp. 566-72.

649 45. *Characterisation and expression analysis of the rainbow trout (Oncorhynchus mykiss) homologue of*
650 *the human dendritic cell marker CD208/lysosomal associated membrane protein 3,.* **Petronella**
651 **Johansson, Yolanda Corripio-Miyar, Tiehui Wang, Bertrand Collet, Chris J. Secombes, Jun Zou.** 3-4,
652 2012, Developmental & Comparative Immunology, Vol. 37, pp. 402-413.

46. *Increased Expression of Ecto-NOX Disulfide-thiol Exchanger 1 (ENOX1) in Diabetic Mice Retina and its Involvement in Diabetic Retinopathy Development.* **YU-CHUEN HUANG, SHIH-PING LIU, SHIH-YIN CHEN, JANE-MING LIN, HUI-JU LIN, YU-JIE LEI, YEH-HAN WANG, WAN-TING HUANG, WEN-LING LIAO, FUU-JEN TSAI.** 6, 2019, In Vivo, Vol. 33, pp. 1801-6.

47. *The plasma membrane nadh oxidase of hela cells has hydroquinone oxidase activity.* **Kishi T, Morre DM, Morre DJ.** 1, 1999, Biochim Biophys Acta, Vol. 1412, pp. 66-77.

48. *CerS6 triggered by high glucose activating the TLR4/IKKβ pathway regulates ferroptosis of LO2 cells through mitochondrial oxidative stress.* **Li D, Tian L, Nan P, Zhang J, Zheng Y, Jia X, Gong Y, Wu Z.** 2023, Mol Cell Endocrinol, Vol. 572, p. 111969.

49. *Evaluating the role of IDO1 macrophages in immunotherapy using scRNA-seq and bulk-seq in colorectal cancer.* **Liu Xingwu, Yan Guanyu, Xu Boyang, Yu Han, An Yue, Sun Mingjun.** 2022, Frontiers in Immunology , Vol. 13.

50. *IDO1 is highly expressed in macrophages of patients in advanced tumour stages of oral squamous cell carcinoma.* **Struckmeier AK, Radermacher A, Fehrenz M, Bellin T, Alansary D, Wartenberg P, Boehm U, Wagner M, Scheller A, Hess J, Moratin J, Freudlsperger C, Hoffmann J, Thurner L, Roemer K, Freier K, Horn D.** 7, 2023, Cancer Res Clin Oncol, Vol. 149, pp. 3623-3635.

51. *IL4i1 and IDO1: Oxidases that control a tryptophan metabolic nexus in cancer.* **Zeitler L, Murray PJ.** 6, 2023, J Biol Chem, Vol. 299, p. 104827.

52. *ALCAM (CD166) is involved in extravasation of monocytes rather than T cells across the blood-brain barrier.* **Lyck R, Lécuyer MA, Abadier M, Wyss CB, Matti C, Rosito M, Enzmann G, Zeis T, Michel L, García Martín AB, Sallusto F, Gosselet F, Deutsch U, Weiner JA, Schaeren-Wiemers N, Prat A, Engelhardt B.** 8, 2017, J Cereb Blood Flow Metab, Vol. 37, pp. 2894-2909.

53. *Cytokine-regulated expression of activated leukocyte cell adhesion molecule (CD166) on monocyte-lineage cells and in rheumatoid arthritis synovium.* **Levesque MC, Heinly CS, Whichard LP, Patel DD.** 12, 1998, Arthritis Rheum, Vol. 41, pp. 2221-9.

54. *Dual role of ALCAM in neuroinflammation and blood-brain barrier homeostasis.* **Lécuyer MA, Saint-Laurent O, Bourbonnière L, Larouche S, Larochelle C, Michel L, Charabati M, Abadier M, Zandee S, Haghayegh Jahromi N, Gowing E, Pittet C, Lyck R, Engelhardt B, Prat A.** 4, 2017, Proc Natl Acad Sci U S A, Vol. 114, pp. E524-E533.

55. *PECAM-1: a multi-functional molecule in inflammation and vascular biology.* **Woodfin A, Voisin MB, Nourshargh S.** 12, 2007, Arterioscler Thromb Vasc Biol, Vol. 27, pp. 2514-23.

56. *Dependence of Mouse Embryonic Stem Cells on Threonine Catabolism.* **al, Jian Wang et.** 2009, Science, Vol. 325, pp. 435-439.

57. *Vitamin B6 Prevents IL-1β Protein Production by Inhibiting NLRP3 Inflammasome Activation.* **Zhang P, Tsuchiya K, Kinoshita T, Kushiyama H, Suidasari S, Hatakeyama M, Imura H, Kato N, Suda T.** 47, 2016, J Biol Chem, Vol. 291, pp. 24517-24527.

58. *Benfotiamine Upregulates Antioxidative System in Activated BV-2 Microglia Cells.* **Bozic I., Savic D., Stevanovic I., Pekovic S., Nedeljkovic N., Lavrnja I.** 9, 2015, Front. Cell. Neurosci, p. 351.

59. *Structural characterisation of inhibitory and non-inhibitory MMP-9–TIMP-1 complexes and implications for regulatory mechanisms of MMP-9.* **Charzewski, Ł., Krzyśko, K.A. & Lesyng, B.** 2021, Sci Rep, Vol. 11, p. 13376.

60. *Matrix metalloproteinase-9: Many shades of function in cardiovascular disease.* **Yabluchanskiy A, Ma Y, Iyer RP, Hall ME, Lindsey ML.** 6, 2013, Physiology (Bethesda), Vol. 28, pp. 391-403.

Tables:

Table 1: Patient demography. Arthritis Type was determined by synovial fluid WBC count per mm^3, %PMNs, and/or culture results. * = 3 patients had Lyme Arthritis, 1 of which had both a S. aureus and positive IgG with confirmatory Western Blot.

Demographics	n=52	
Age	(years)	
	Mean (STD)	51.7 (21)
	Median	58
	Range	3-77
Gender	n, (%)	
	Male	35 (68)
	Female	17 (32)
Race and Ethnicity	n, (%); Hispanic n, (%)	
	White	45 (87); 1 (2)
	Black	3 (6); 0
	Asian	1 (2); 0
	Multiracial	1 (2); 0
	Unknown	1 (2); 0
Arthritis Type	n (%)	
	Normal/Non-I	9 (25)
	Inflammatory	8 (22)
	Septic*	18 (50)
	Hemorrhagic	1 (3)

Figures:

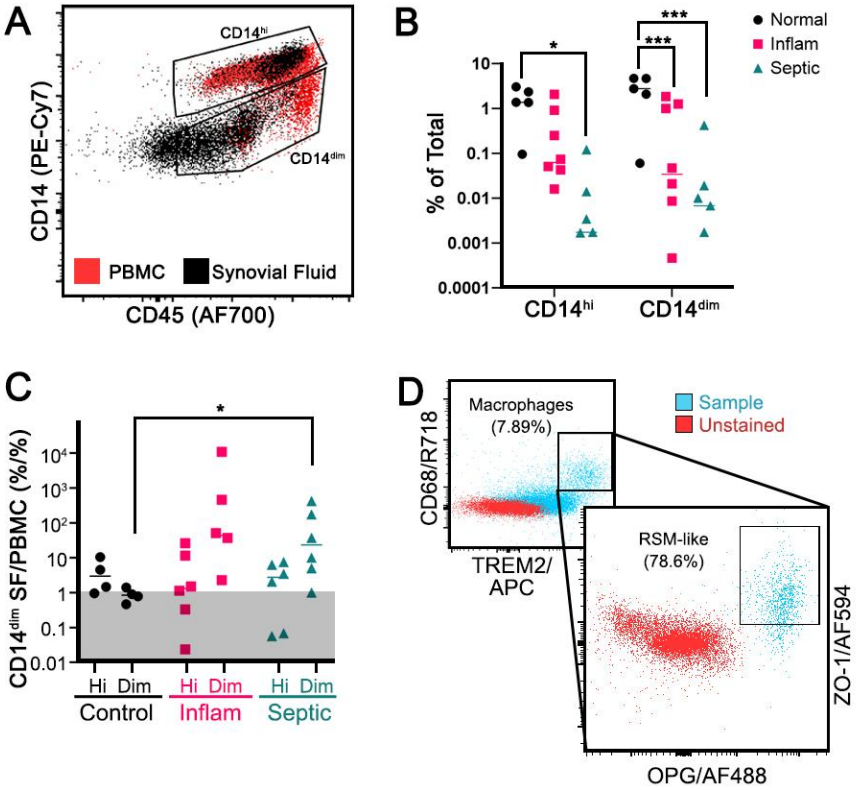

Figure 1: Resident Synovial Macrophage-like cells. Live, CD56$^-$CD3$^-$CD20$^-$RANKL$^-$CD11c$^-$TREM2$^+$OPG$^+$CD68$^+$CD11b$^+$HLA-DR$^+$CX3CR1$^+$ cells were identified with an enrichment of CD14^{dim} cells in the SF compared to PBMCs (**A**, n=6 patients for preliminary evaluation for RSM cells). These CD14^{dim} macrophages were decreased in absolute frequency inflammatory and septic arthritis compared to controls (**B**, n=16 patients, 4-6 patients per group) but were relatively enriched in the SF of septic joints when SF cells were compared to PBMC (**C**, n=16 patients, 4-6 patients per group). Back-gating on the Alive/CD14^{dim} population to identify M2 macrophages (D, inset), 78.6% were double positive for OPG and ZO-1 (**D**, representative patient with inflammatory arthritis). Two-way ANOVA with Tukey's *post-hoc* correction. *p <0.05; ***p<0.001

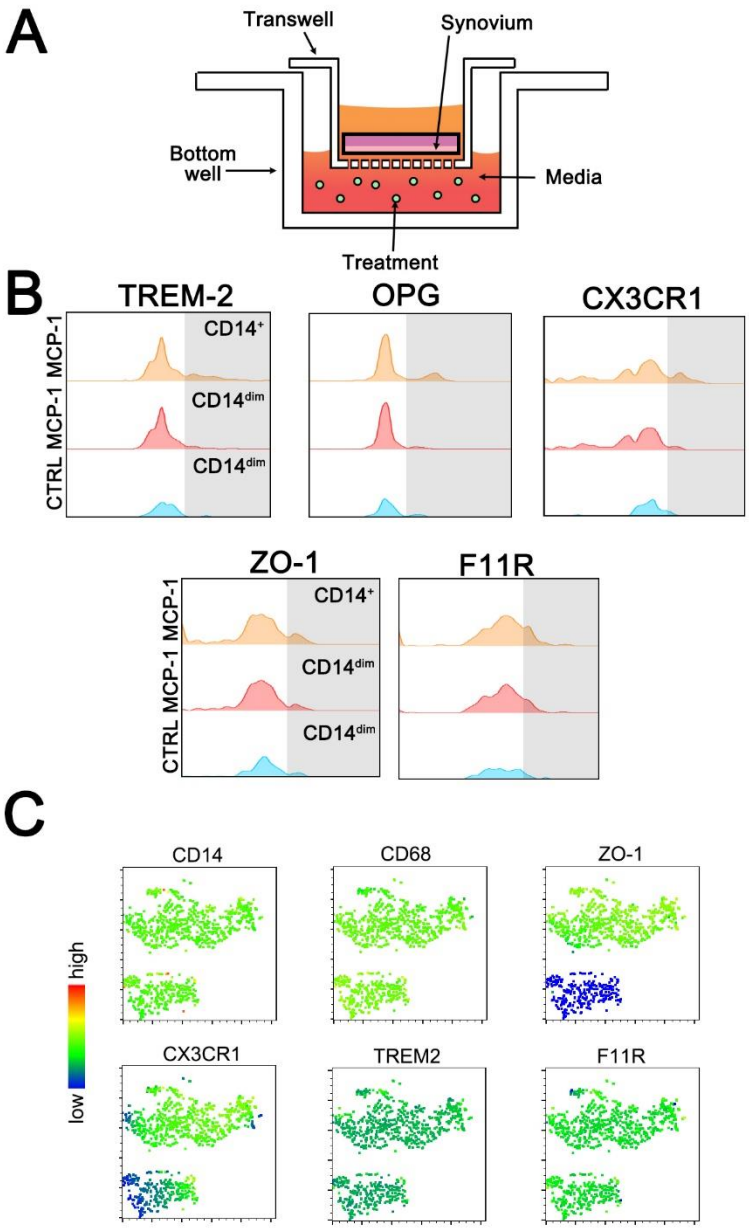

Figure 2: Transwell synovial cell migration assay. Schematic of the experimental set up (**A**). Resident synovial macrophage markers TREM-2+, OPG+, CX3CR1+, ZO-1+ and F11R+ were evaluated within the migratory monocyte/macrophage population (Alive/CD56-/CD3-/CD11c-/CD20-/CD14+/CD11b+) in a representative patient treated with 250 ng/mL of MCP-1 (**B**). tSNE plots of the same patient's migratory myeloid cells demonstrating ZO-1 has the most delineation from other markers (**C**).

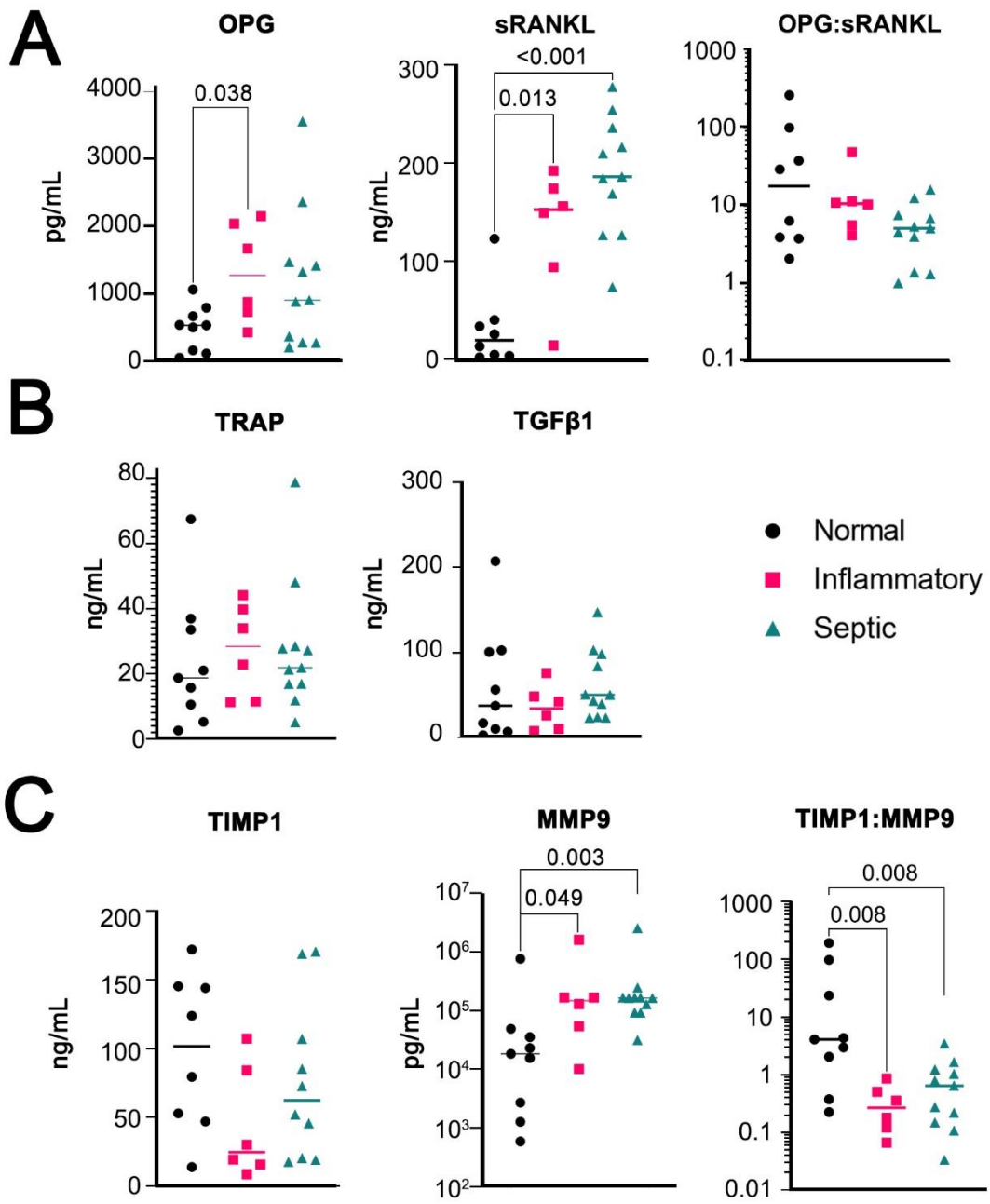

Figure 3: ELISA results of SF supernatant protein concentration. OPG, sRANKL, and ratio of OPG:sRANKL (A). TRAP and TGF-β1, (B). Measures of TIMP1, MMP9, or ratio of TIMP1:MMP9. Normal (n=9), inflammatory (n=6), and septic (n=11). Multiple Mann-Whitney tests with FDR rate <0.05.

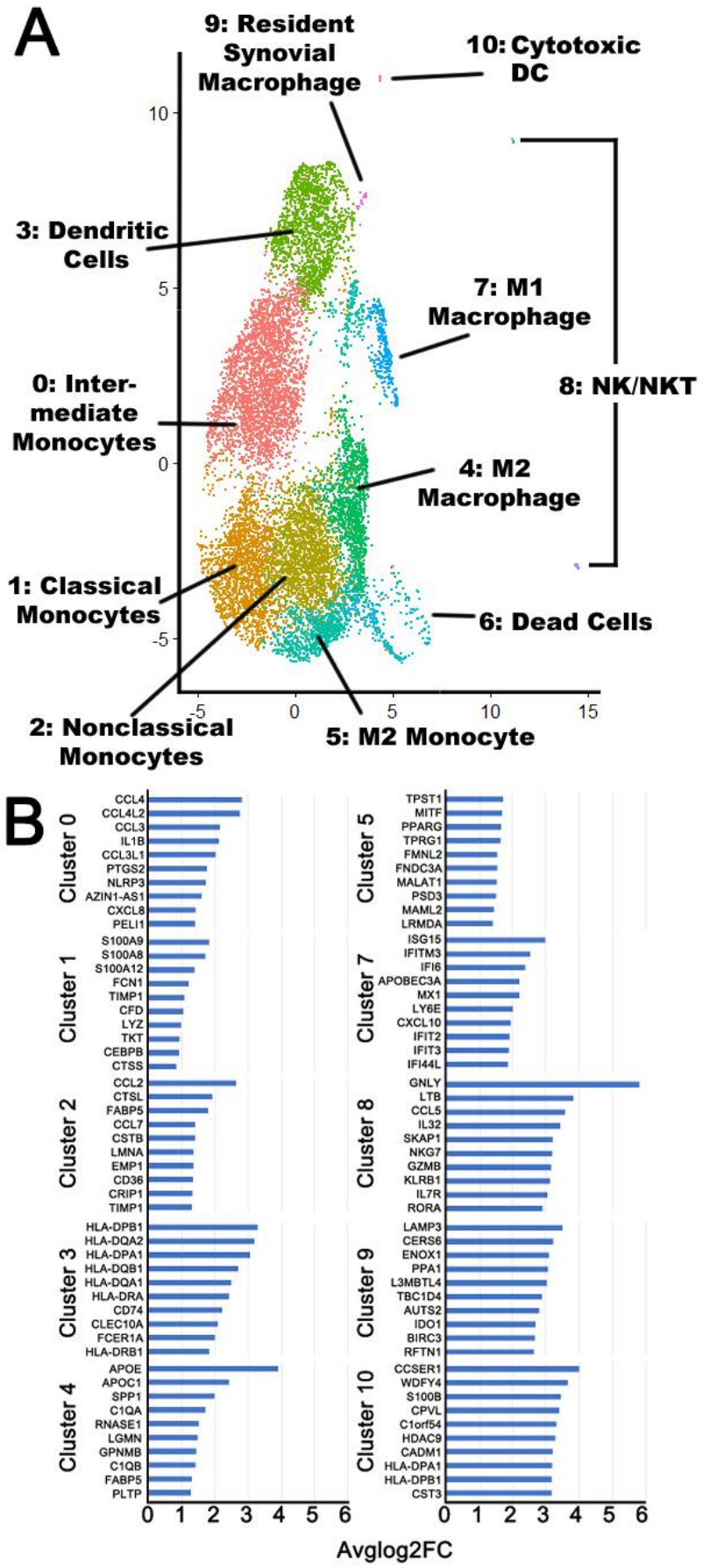
A
9: Resident Synovial Macrophage
10: Cytotoxic DC
3: Dendritic Cells
7: M1 Macrophage
8: NK/NKT
0: Inter-mediate Monocytes
4: M2 Macrophage
1: Classical Monocytes
6: Dead Cells
2: Nonclassical Monocytes
5: M2 Monocyte
B
Cluster 0
CCL4
CCL4L2
CCL3
IL1B
CCL3L1
PTGS2
NLRP3
AZIN1-AS1
CXCL8
PELI1
Cluster 1
S100A9
S100A8
S100A12
FCN1
TIMP1
CFD
LYZ
TKT
CEBPB
CTSS
Cluster 2
CCL2
CTSL
FABP5
CCL7
CSTB
LMNA
EMP1
CD36
CRIP1
TIMP1
Cluster 3
HLA-DPB1
HLA-DQA2
HLA-DPA1
HLA-DQB1
HLA-DQA1
HLA-DRA
CD74
CLEC10A
FCER1A
HLA-DRB1
Cluster 4
APOE
APOC1
SPP1
C1QA
RNASE1
LGMN
GPNMB
C1QB
FABP5
PLTP
Cluster 5
TPST1
MITF
PPARG
TPRG1
FMNL2
FNDC3A
MALAT1
PSD3
MAML2
LRMDA
Cluster 7
ISG15
IFITM3
IFI6
APOBEC3A
MX1
LY6E
CXCL10
IFIT2
IFIT3
IFI44L
Cluster 8
GNLY
LTB
CCL5
IL32
SKAP1
NKG7
GZMB
KLRB1
IL7R
RORA
Cluster 9
LAMP3
CERS6
ENOX1
PPA1
L3MBTL4
TBC1D4
AUTS2
IDO1
BIRC3
RFTN1
Cluster 10
CCSER1
WDFY4
S100B
CPVL
C1orf54
HDAC9
CADM1
HLA-DPA1
HLA-DPB1
CST3
0 1 2 3 4 5 6
Avglog2FC

Figure 4: Unsupervised Cluster Analysis showing composite of 3 patients with inflammatory arthritis (A). Clusters were manually identified based on top ten expressed genes (B) in addition to classical markers. Analysis performed in R with resolution of 0.4 and dimensions 1:30. N = 3 patients per inflammatory and septic arthritis.

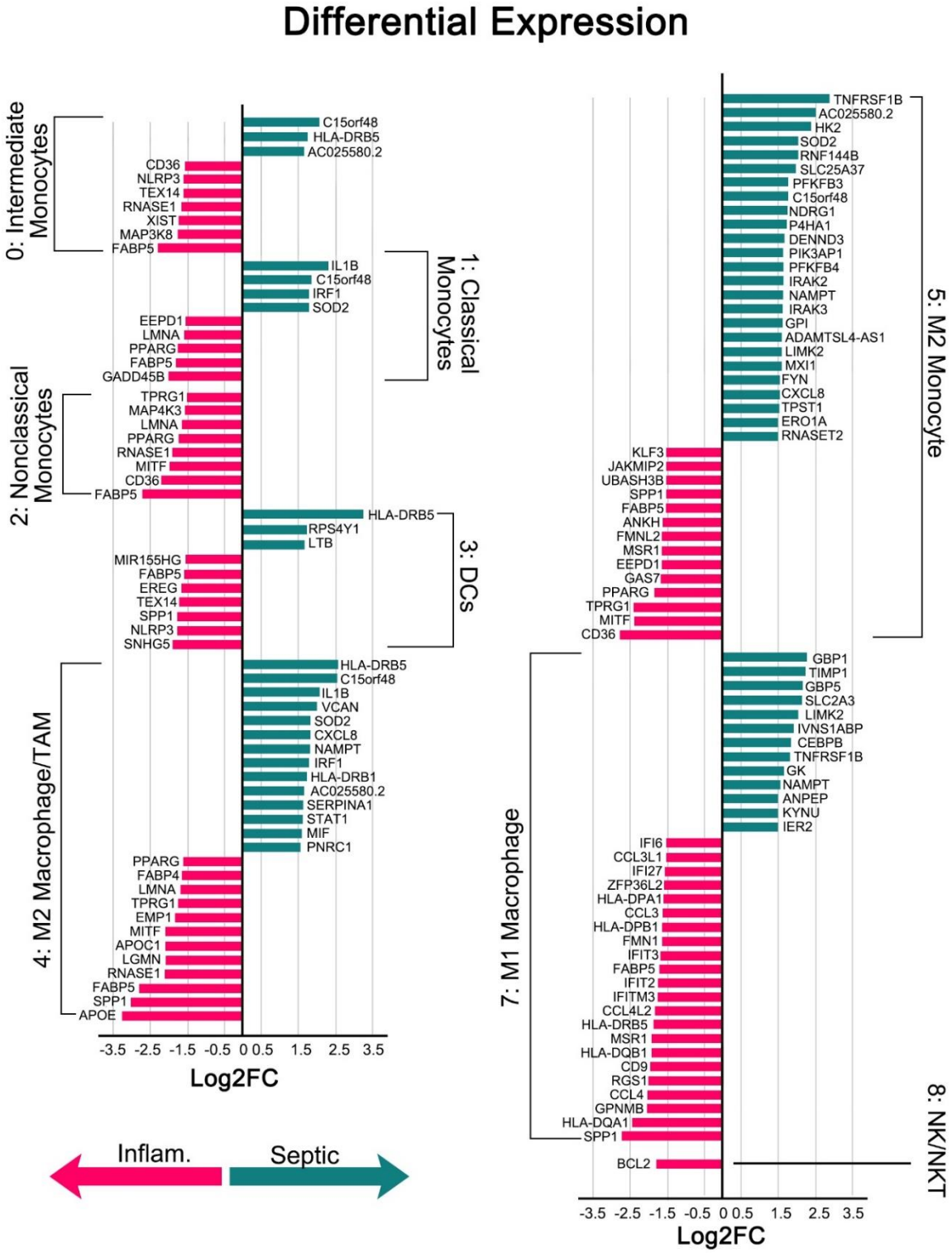

Figure 5: Differentially Expressed Genes (DEGs) where Log2FC > 1.5. Frame of reference is from septic arthritis (identity 1) compared inflammatory arthritis (identity 2).

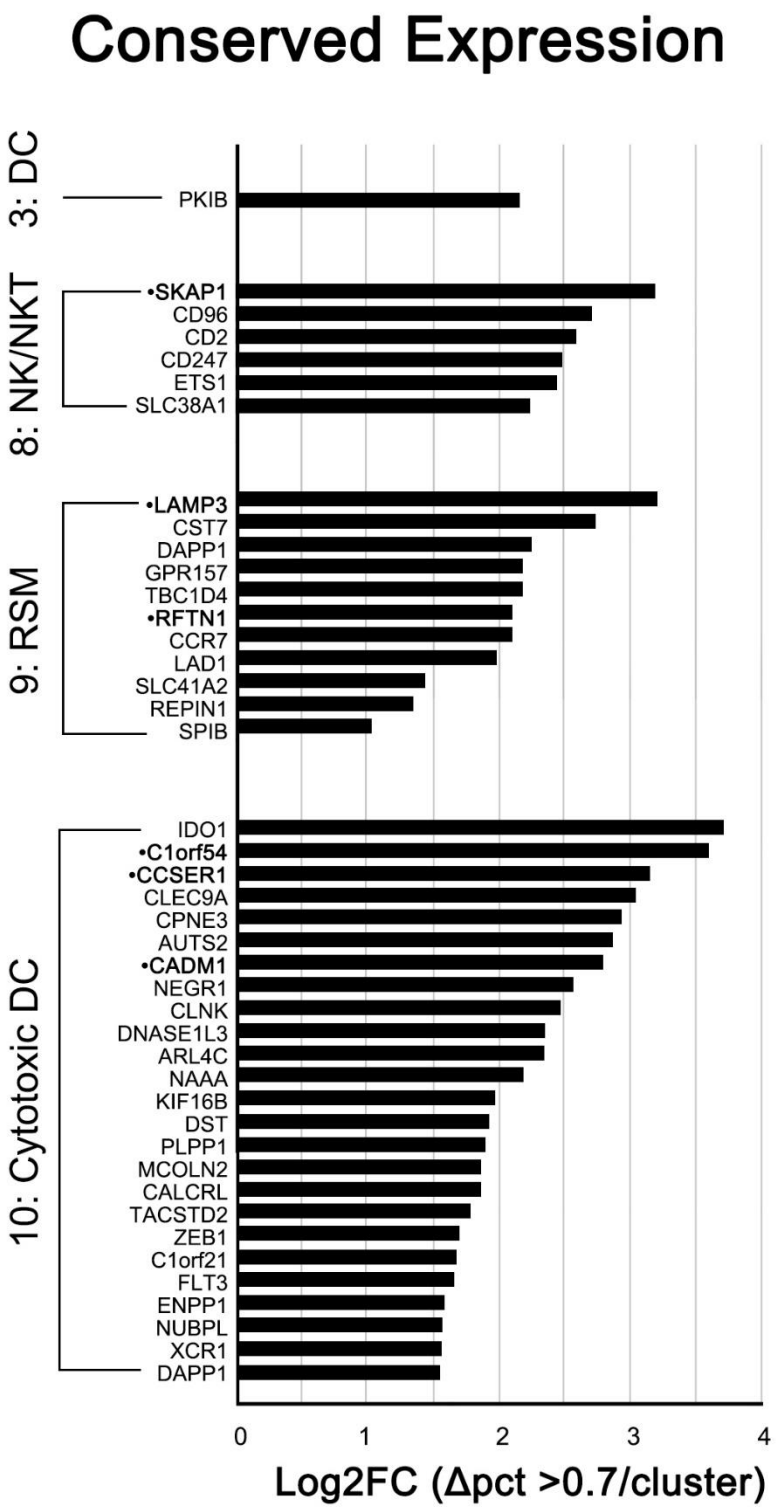

Figure 6: Conserved genes where Log2FC > 1.5 and the change in percent expression in both septic arthritis and inflammatory arthritis was > 0.7 in each cluster compared to all other clusters. Gene names in **•bold** represent genes that were also in the top 10 expressed genes in **Figure 4**.

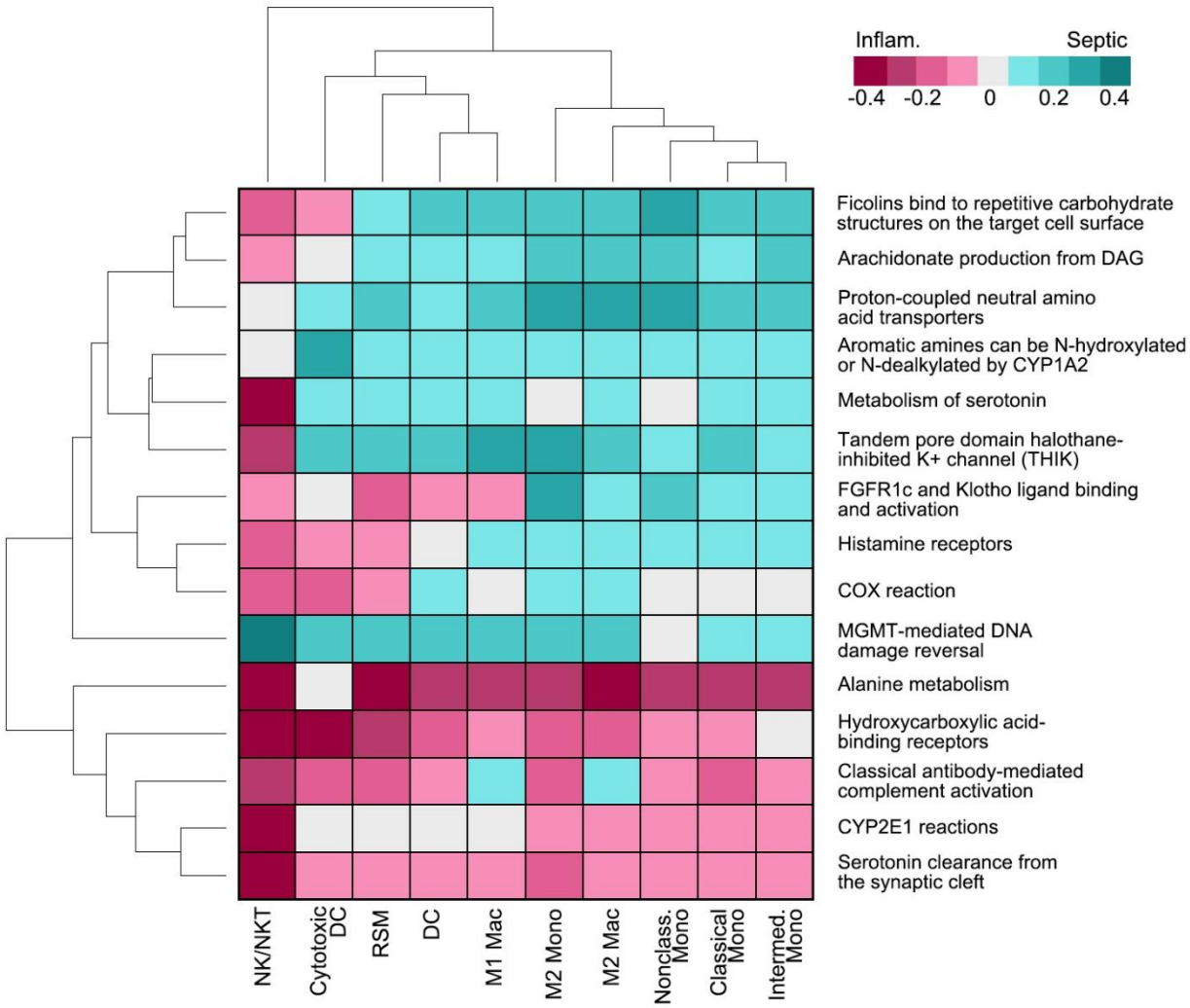

Figure 7: Top 15 most up or downregulated pathways using DEGs and ReactomeGSA.

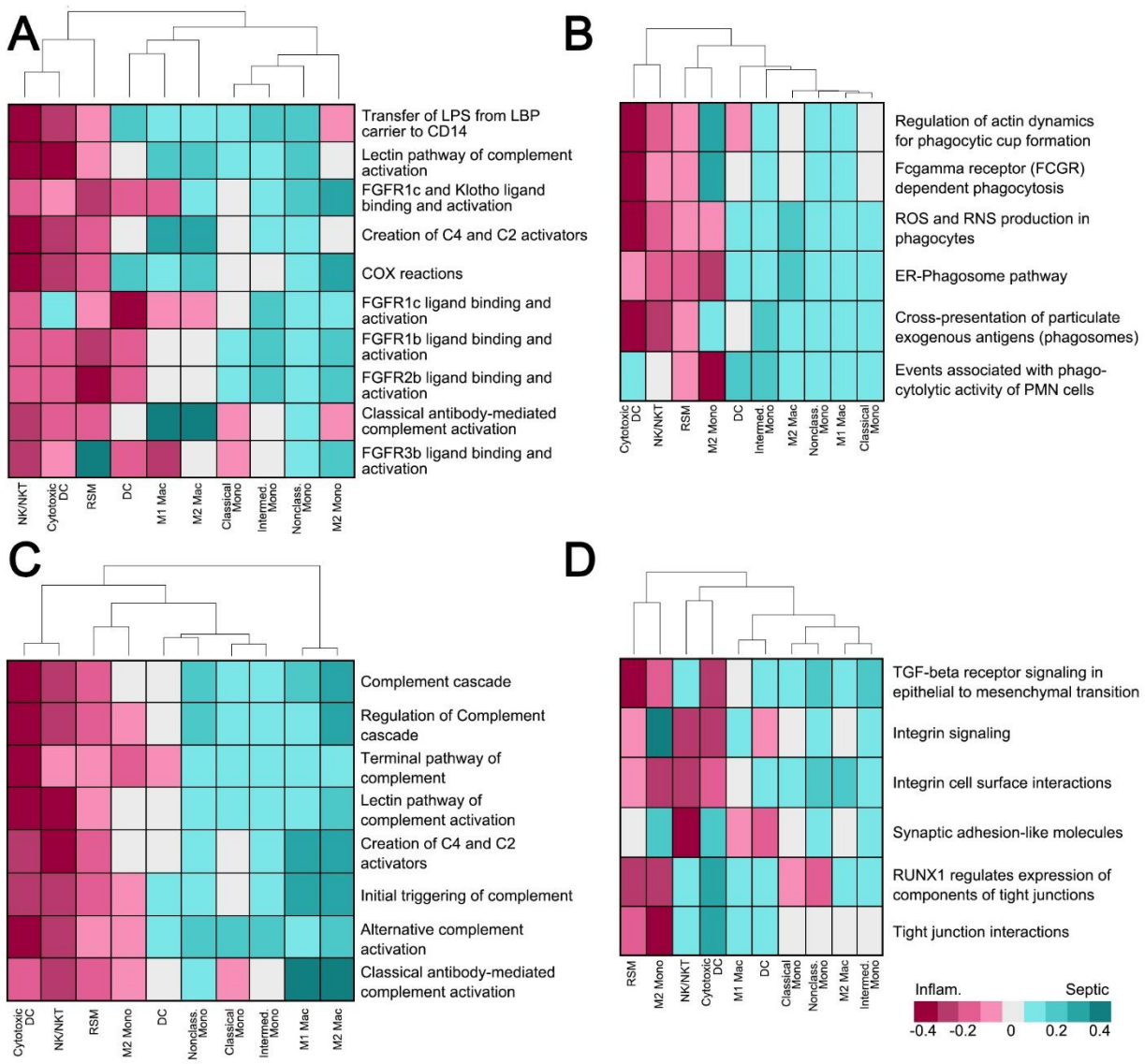

Figure 8: Functional analysis of clusters by top 10 immune relevant pathways (A), all searchable phagocytosis terms (B), all searchable complement terms (C), and all searchable adhesion/integrin signaling terms (D).

Supplementary Table 1: Flow cytometry panels used in Figure 1 (top) and modified panel used after Figure 1 (bottom).

Molecular Target	Fluorochrome	Clone	Vendor	Cell of Interest
TREM2	APC	237920	R&D Systems	Macrophage
RANKL/TNFSF11	AF350	685857	R&D Systems	OB/activated T cells
OPG/TNFRSF11B	AF488	155321	R&D Systems	RSM
CD11b	BV605	ICRF44	BioLegend	Myeloid
CD14	PE-Cy7	63D3	BioLegend	Mac/Mono
CD45	AF700	2D1	BioLegend	Leukocytes
HLA-DR	PE	Tu36	BioLegend	Activated APC
CX3CR1	BV421	2A9-1	BioLegend	RSM/Mac/Mono
CD68	PerCP-Cy5.5	Y1/82A	BioLegend	Macrophage
CD3	BV650	UCHT1	BioLegend	T Cell
CD56	PE-Cy5	5.1H11	BioLegend	NK cell
CD20	BV785	2H7	BioLegend	B cell
CD11c	BV785	3.9	BioLegend	Dendritic Cell

Molecular Target	Fluorochrome	Clone	Vendor	Cell of Interest
TREM2	APC	237920	R&D Systems	Macrophage
RANKL/TNFSF11	PE	MIH24	BioLegend	OB/activated T cells
OPG/TNFRSF11B	AF488	155321	R&D Systems	RSM
CD11b	BV605	ICRF44	BioLegend	Myeloid
CD14	PE-Cy7	63D3	BioLegend	Mac/Mono
CD45	AF532	AF532	ThermoFisher	Leukocytes
HLA-DR	APC-Fire 810	L243	BioLegend	Activated APC
CX3CR1	BV711	2A9-1	BioLegend	RSM/Mac/Mono
CD68	R718	Y1/82A	BD Biosciences	Macrophage
CD3	BV650	UCHT1	BioLegend	T Cell
CD56	BUV737	NCAM16.1	BD Biosciences	NK cell
CD20	BUV805	2H7	BD Biosciences	B cell
CD11c	BUV615	3.9	BD Biosciences	Dendritic Cell
ZO-1/TJP1	AF594	polyclonal	ThermoFisher	RSM
F11R/JAM-1	BV421	M.Ab.F11	BD Biosciences	RSM

Supplementary Table 2: Patient Diagnosis. SF analysis was performed on patients when it was clinically indicated. SF diagnosis was based on WBC count (# nucleated cells) and % PMN based on neutrophil count. * = not performed. ** = Lyme Arthritis in addition to other bacterial arthritis.

Patient	Color	Clarity	Crystals	# Nucleated Cells	# Neutrophils	# Lymphocytes	Arthritis Type
2	Red	Turbid	CCP, MSU	29783	22635	101	Inflammatory
3	Yellow	Turbid	CPP	4716	2453	20	Inflammatory
5	Red	Turbid	none	822	674	107	Non-Inflammatory
6	Yellow	Turbid	none	29497	28022	0	Septic
7	Yellow	Hazy	none	714	29	64	Non-Inflammatory
9	Yellow	Hazy	none	63726	60539	1275	Septic
10	Yellow	Slightly Hazy	none	464	28	70	Non-Inflammatory
11	Red	Turbid	none	671	658	0	Non-Inflammatory
13	Orange	Hazy	none	831	632	58	Non-Inflammatory
14	None	Clear	none	29	0	7	Normal
15	Orange	Turbid	none	63184	60025	632	Inflammatory
16	Pink	Hazy	none	166627	128303	9998	Septic
18	Amber	Turbid	none	134280	119509	2686	Septic
19	Red	Turbid	none	11522	8987	1959	Inflammatory
21	N/A	N/A	none	N/A	N/A	N/A	Septic
22	Yellow	Turbid	CPP	34482	27586	2	Inflammatory
23	Yellow	Clear	none	348	28	52	Non-Inflammatory
24	Red	Turbid	none	1819	1564	14	Hemorrhagic
26	Yellow	Clear	none	26	5	12	Normal
27	Orange	Turbid	MSU	33805	26030	0	Inflammatory
28	Brown	Turbid	none	66945	*	*	Septic
30	Yellow	Slightly Hazy	none	26536	25209	531	Septic
31	Red	Hazy	none	48363	46428	484	Septic
32	Orange	Hazy	none	43355	42054	434	Septic
33	Red	Turbid	none	304	76	85	Septic
34	Red	Hazy	none	854	384	154	Non-Inflammatory
38	Red	Turbid	none	114000	1000320	2	Septic
39	Red	Turbid	MSU	76890	76121	0	Inflammatory
40	Pale Yellow	Turbid	CPP	67368	64673	0	Inflammatory
41	Pink	Turbid	None	79118	75162	0	Septic**
43	Orange	Turbid	None	104595	92044	2	Septic
46	Pink	Turbid	None	80562	74117	2417	Septic
47	Red	Turbid	None	9884	8303	692	Septic
48	Orange	Hazy	None	130	83	26	Normal
49	Yellow	Hazy	MSU	20566	18715	0	Inflammatory

Supplementary Table 3: List of all significant conserved genes in RSM, Cytotoxic DC, and NK/NKT clusters.

Gene	Log2FC	Δ % Septic	Δ % Inflam	Cluster	Gene Function
PKIB	2.10657	0.71	0.726	DC	Also known as AKT, causes M2 formation
SKAP1	3.16933	0.89	0.954	NK/NKT	TCR adaptor protein
CD96	2.690931	0.77	0.874	NK/NKT	Inhibitory, marker of exhaustion
CD2	2.571958	0.78	0.817	NK/NKT	Regulates lytic activity
CD247	2.473159	0.79	0.869	NK/NKT	Subunit of T cell antigen receptor complex
ETS1	2.430819	0.85	0.88	NK/NKT	Required for NK differentiation and cytotoxic function
SLC38A1	2.222173	0.82	0.77	NK/NKT	Glutamine transporter
IDO1	3.679276	0.93	0.764	Cytotoxic DC	Immunosuppressive, expressed by DCs, macs, and epithelial cells
C1orf54	3.555745	0.94	0.794	Cytotoxic DC	cDC1 gene
CCSER1	3.110627	0.78	0.818	Cytotoxic DC	upregulated in anti-inflammatory conditions
CLEC9A	3.009585	1.00	0.888	Cytotoxic DC	DC receptor for necrotic cell death
CPNE3	2.908024	0.82	0.76	Cytotoxic DC	cDC1 gene
AUTS2	2.836438	0.78	0.74	Cytotoxic DC	associated with autism
CADM1	2.766723	0.99	0.936	Cytotoxic DC	expressed by pre-cDC1, cell adhesion
NEGR1	2.54191	0.97	0.798	Cytotoxic DC	immunoglobulin superfamily cell adhesion molecule subgroup IgLON, has been implicated in neuronal growth and connectivity
CLNK	2.441584	0.99	0.885	Cytotoxic DC	upregulated in response to IL-2 and IL-3, associated with SLP-76
DNASE1L3	2.326661	0.89	0.998	Cytotoxic DC	Cytokine secretion following inflammasome activation in response to DNA in circulating apoptotic bodies
ARL4C	2.315802	0.71	0.709	Cytotoxic DC	oncogene, tubulogenesis, wnt-beta catenin signaling
NAAA	2.166039	0.71	0.78	Cytotoxic DC	inflammatory, lysosomal
KIF16B	1.944567	0.79	0.778	Cytotoxic DC	microtubule formation associated with endosomes and cross presentation
DST	1.91132	0.77	0.764	Cytotoxic DC	junctional adhesion protein

PLPP1	1.872874	0.74	0.736	Cytotoxic DC	phospholipid lipase associated with mac inflammation, cDC1 marker
MCOLN2	1.841604	0.73	0.824	Cytotoxic DC	MHCII presentation, innate immune cell activation, enhances infectivity of certain viruses, interferon stimulating gene
CALCRL	1.840268	0.76	0.951	Cytotoxic DC	regulates DC function through NF-kB
TACSTD2	1.765963	0.78	0.989	Cytotoxic DC	Marker for TGF-B1 dependent DCs
ZEB1	1.672937	0.74	0.941	Cytotoxic DC	cDC1 cells
C1orf21	1.647088	0.84	0.9	Cytotoxic DC	enriched in cytotoxic CD8 T cells
FLT3	1.645133	0.96	0.895	Cytotoxic DC	The growth factor Flt3 ligand (Flt3L) is central to dendritic cell (DC) homeostasis and development, controlling survival and expansion by binding to Flt3 receptor tyrosine kinase on the surface of DCs.
ENPP1	1.548458	1.00	0.777	Cytotoxic DC	suppresses innate immune response,
NUBPL	1.540362	0.83	0.911	Cytotoxic DC	mitochondrial gene, iron and sulfur
XCR1	1.53506	0.78	0.995	Cytotoxic DC	DC, induces CD8 responses
DAPP1	1.52997	0.72	0.717	Cytotoxic DC	immune related mucosal tissues, hyper-reactive airway disease, IDO1/CCR7 signaling, associated with DCs
LAMP3	3.181144	0.88	0.967	RSM	lysosome
CST7	2.710421	0.93	0.748	RSM	Cistatin F, lysosomal cathepsin inhibitor
DAPP1	2.225168	0.72	0.781	RSM	immune related mucosal tissues, hyper-reactive airway disease, IDO1/CCR7 signaling, associated with DCs
GPR157	2.163834	0.75	0.897	RSM	G protein coupled receptor 157
TBC1D4	2.161417	0.79	0.941	RSM	Rab GTPase Activating Protein
RFTN1	2.085313	0.77	0.736	RSM	glucose transport
CCR7	2.083676	0.92	0.837	RSM	M1 polarization
LAD1	1.96187	0.77	0.713	RSM	epithelialization
SLC41A2	1.415962	0.76	0.78	RSM	magnesium transporter
REPIN1	1.325367	0.76	0.72	RSM	increasing cell size and tumor metastasis
SPIB	1.005641	0.75	0.726	RSM	recruits TAMs via CCL4 signaling

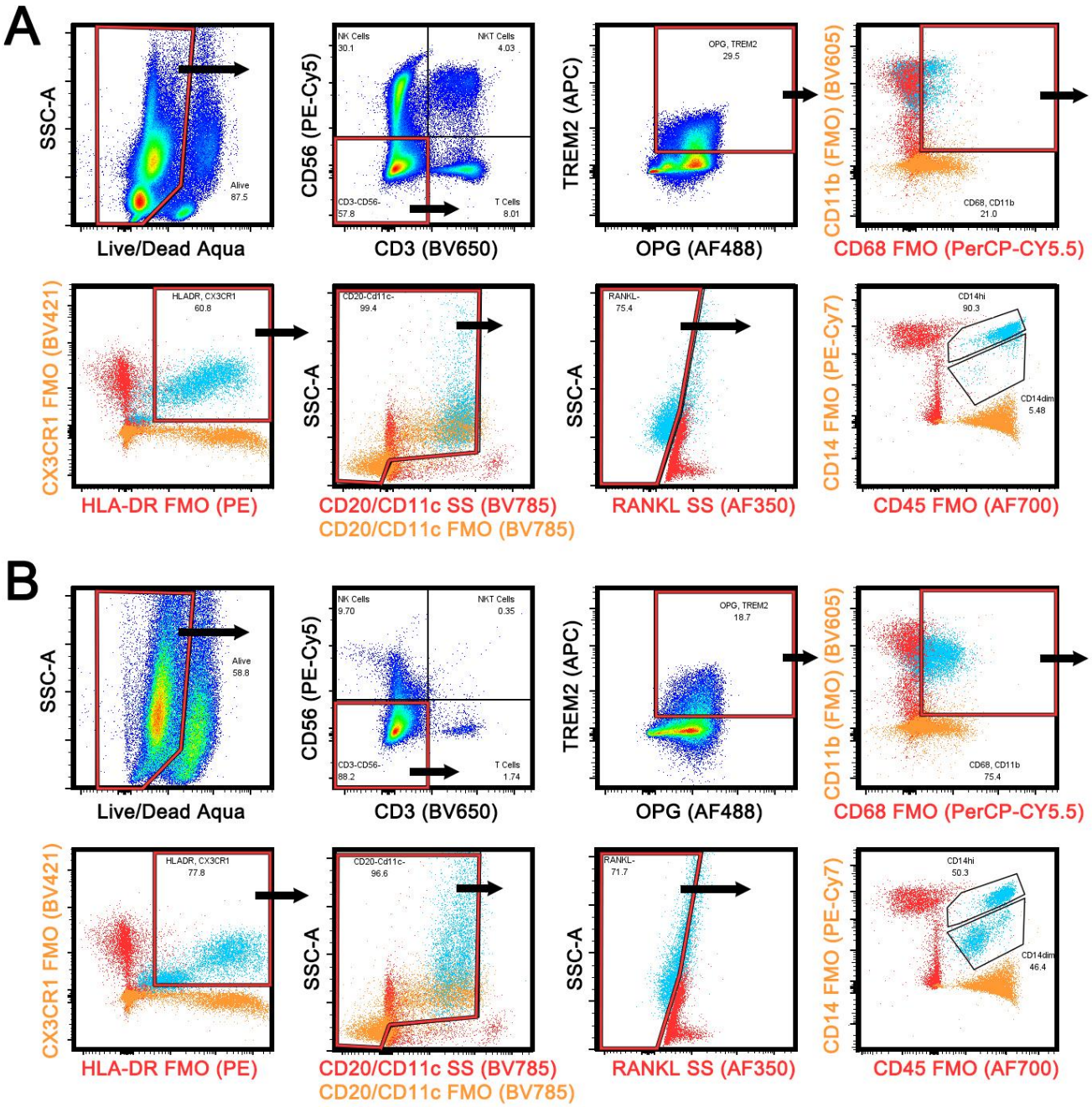

Supplemental Figure 1: Initial discovery of viable CD14^{dim} TREM2^{+}OPG^{+} macrophages consistent with RSM in SF and enriched compared to matched PBMC sample. Gating of PBMCs (**A**) and SF cells (**B**). FMO controls shown where discrete populations were not available for gating.

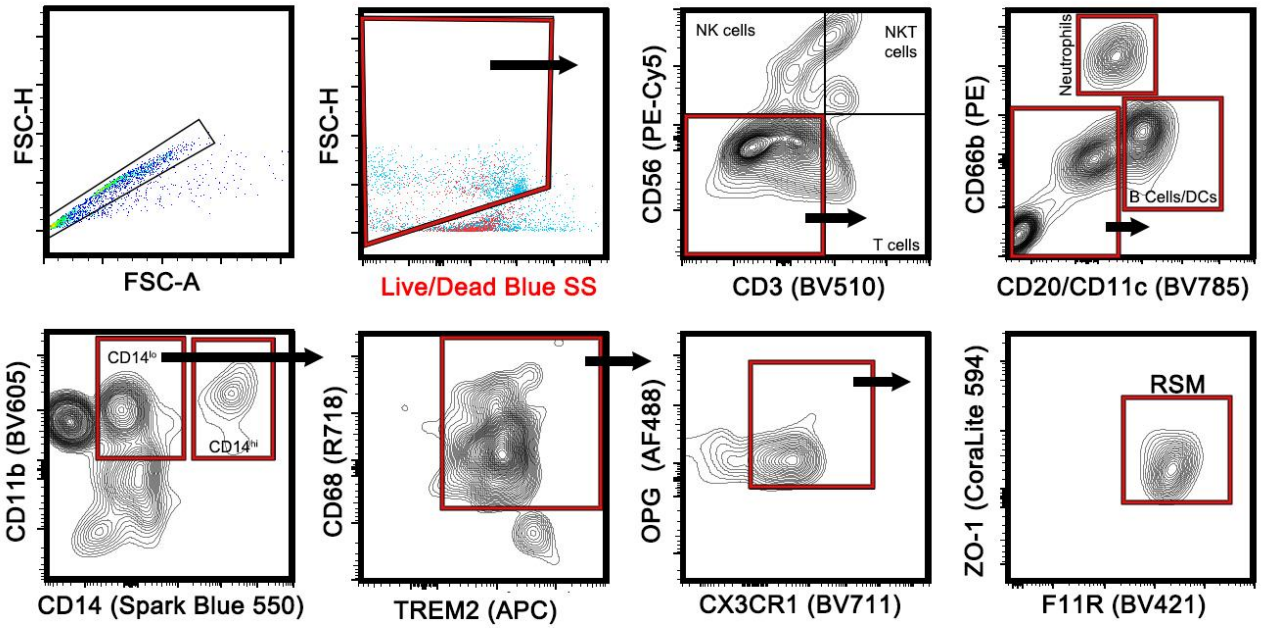

Supplemental Figure 2: Gating of migratory cells from synovium into the bottom transwell to identify $CD14^{dim+}TREM2^{+}CX3CR1^{+}OPG^{+}F11R^{+}ZO\text{-}1^{+}$ macrophages consistent with RSM. Live/Dead single stain (red) shown over sample (blue) in second image.

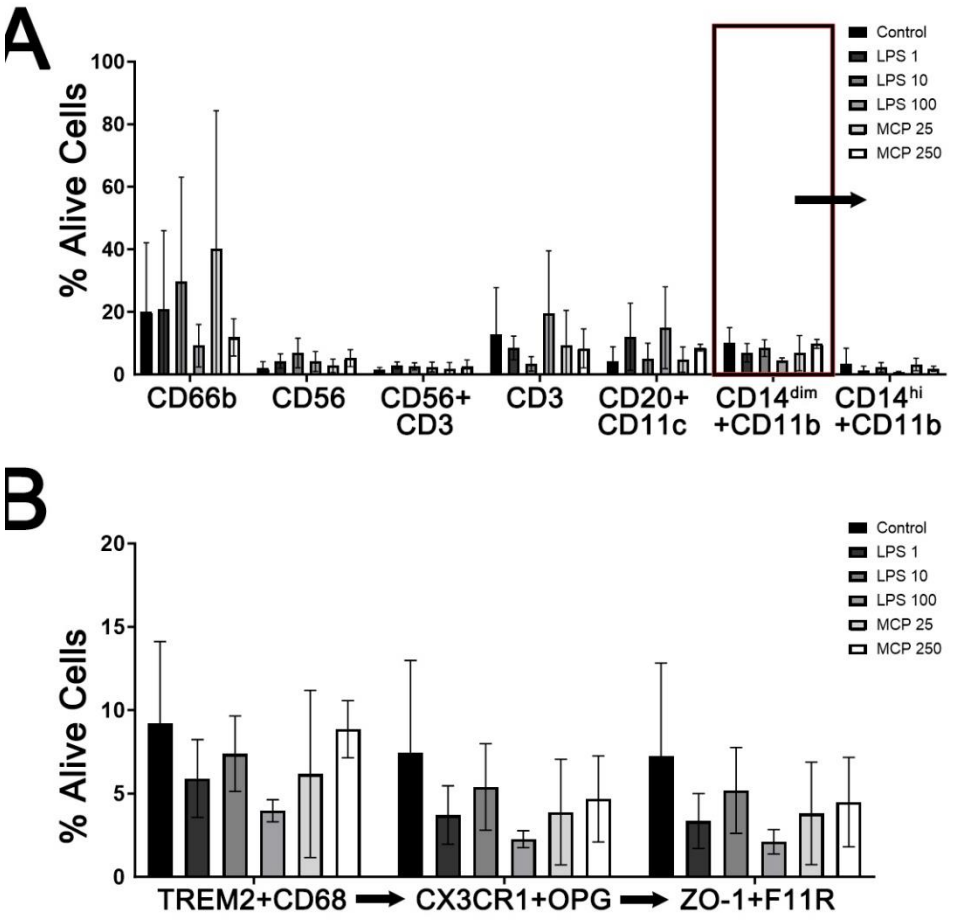

Supplementary Figure 3: Evaluation of migratory cell populations in the bottom transwell. Neutrophils (CD66b), NK (CD56), NKT (CD3 and CD56), T cells (CD3), B cells or Dendritic Cells (CD20 and CD11c, same fluorophore), and CD14 high or dim myeloid (CD11b) cells (**A**). Sequential analysis of the $CD14^{dim}$ myeloid population demonstrating nearly all $CD14^{dim}$ macrophages are positive for OPG, CX3CR1, ZO-1, and F11R (**B**). LPS in µg/mL, MCP-1 in ng/mL.

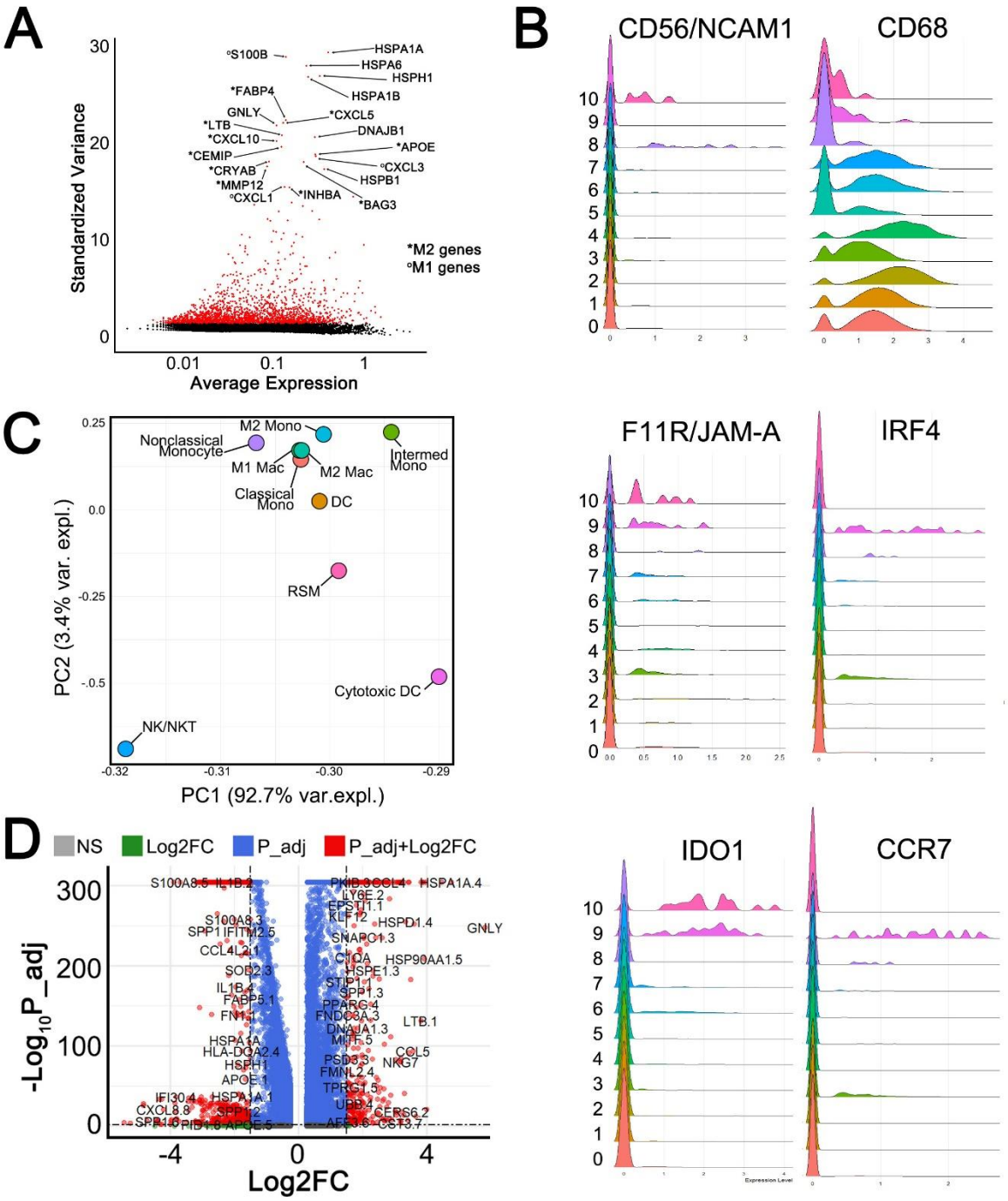

Supplemental Figure 4: Evaluation of scRNA-seq data. Variance analysis with top 20 genes labeled (A). Ridge plots of NK, M2, and RSM associated genes (B). Principle component analysis of all 10 clusters not including dead cells (C). Volcano plot of most up- and down-regulated genes, where minimum Log2FC was 1.5 for significance given homogeneity of sample (D).

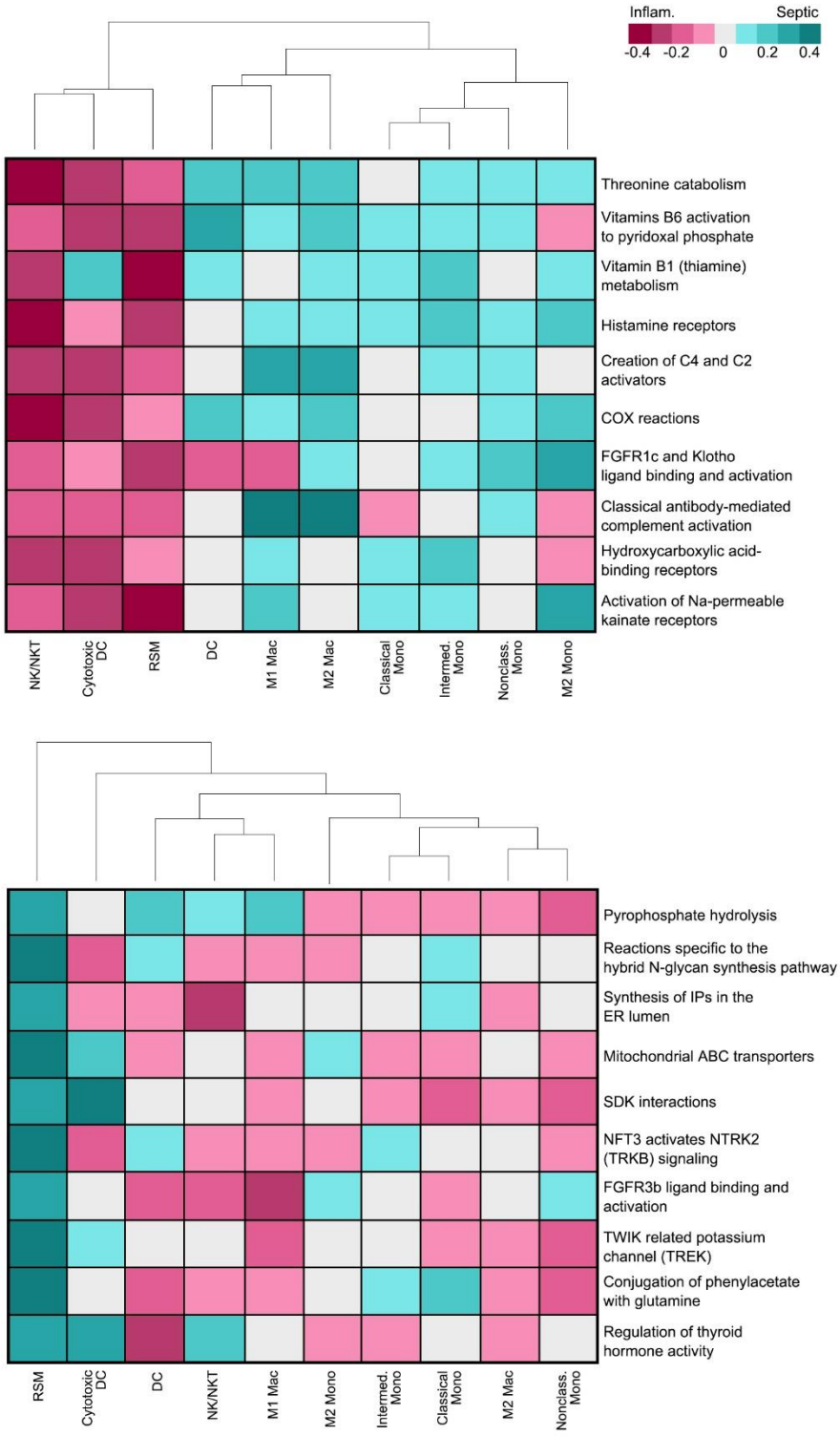

Supplemental Figure 5: GSA for RSMs: top ten genes upregulated in inflammatory arthritis (top) and septic arthritis (bottom).